ψ

X-692-74-216
PREPRINT

NASA TM X- 70714

INTERPLANETARY STREAMS AND THEIR INTERACTION WITH THE EARTH

(NASA-TM-X-70714) INTERPLANTETARY STREAMS AND THEIR INTERACTION WITH THE EARTH (NASA) 60 p HC $6.00 CSCL 03B
N74-30258
Unclas
G3/29 54791

L. F. BURLAGA

JULY 1974

GSFC
GODDARD SPACE FLIGHT CENTER
GREENBELT, MARYLAND

Interplanetary Streams and their Interaction with the Earth

By

L. F. Burlaga
NASA/Goddard Space Flight Center
Laboratory for Extraterrestrial Physics
Greenbelt, Maryland

TABLE OF CONTENTS

Interplanetary Streams and their Interaction with the Earth

Abstract

Plasma and magnetic field observations of interplanetary streams near 1 AU are summarized. Two types of streams have been identified—corotating streams and flare-associated, and other flow patterns are present due to interactions among streams. The theory of corotating streams, which attributes them to a high temperature region near the Sun, satisfactorily explains many of the effects observed at 1 AU. A correspondingly complete theory of flare-associated streams does not exist. Streams are a key link in the chain that connects solar and geomagnetic activity. The factors that most influence geomagnetic activity are probably related to streams and determined by the dynamics of streams. The evolution of streams on scales of 27 days and 11 years probably determines the corresponding variations of geomagnetic activity.

1.0 Introduction

Joint interplanetary and geomagnetic studies have contributed much to our understanding of the solar wind as well as to our understanding of geomagnetic activity. A particularly good example of a subject which has grown as a result of the interaction between these two disciplines is the subject of interplanetary streams. Numerous investigations of geomagnetic activity, reviewed by Akasofu and Chapman (1972) consistently revealed two general kinds of disturbances. One includes a discontinuous increase in the horizontal component of the geomagnetic field, lasts for several days, and tends to follow a large flare. The other type of disturbance also lasts for days, but it is less intense, does not usually follow a flare, and recurs one or more times at 27 day intervals. These two types of disturbances are called SSC events (storm sudden commencements) and recurrent storms, respectively. SSC events were attributed to interplanetary streams (alias jets, solar shells, pistons, nascent streams) which were presumed to be emitted by solar flares. Recurrent storms were attributed to long-lived, interplanetary streams emanating from unidentified regions on the sun which were labeled M-regions (Bartels, 1932; Chapman, 1964). A third type of interplanetary flow, the "quiet wind," was postulated to explain the continual presence of comet tails (e.g., Chapman, 1964). Gas dynamic models of such flows were reviewed by Parker (1963). The in-situ measurements of the solar wind, beginning in 1962, confirmed the existence of these three types of flows. Theoretical studies related to the early measurements concentrated on steady-state models of the "quiet wind" and extensions of Parker's work on shock waves. This work was reviewed by Hundhausen (1972a) at the last STP meeting. Since 1970, there has been a rapid expansion of our knowledge of streams, both experimental and theoretical. These results form the bulk of this review. There has been a corresponding growth of our understanding of the physical processes involved in the solar wind-magnetosphere interaction, and of the solar wind parameters which are most important in producing geomagnetic activity, based mainly on statistical, correlative studies (e.g., see the reviews by Kovalevsky, 1971; and Svalgaard, 1973), but this work will not be reviewed here. The problem of relating the physical parameters that produce geomagnetic activity to the physical processes and the configurations in the solar wind has not been solved. Work on this problem, especially on the relations between streams and geomagnetic activity, is reviewed in Section 5.

2.0 Classification of Streams

Some general features of the solar wind flow are illustrated in Figure 1, which shows daily averages of the bulk speed V(t), proton density, n(t), magnetic field intensity, B(t), and sign of the magnetic field direction (toward (+) the sun or away (-)); the data are from the Solar Terrestrial Activity Chart for 1968, compiled by Obayashi. One does not see simple, isolated streams imbedded in a "quiet" solar wind flow ("quiet wind" corresponding, e.g., to 300 km/sec-350 km/sec, as defined by Hundhausen, 1972b). Rather, quiet wind flows are few, and they rarely persist for more than two days, while there are many kinds of high-speed flow patterns that might be called streams, many of which seem to be contiguous of even superimposed on one another. Burlaga and Ogilvie (1973) distinguished three kinds of patterns in the velocity profile:

Simple Stream - This has two parts, the "rise" and the "decline". The rise is characterized by a smooth increase of the bulk speed from V_{min} to a maximum value, V_{max}. At 1 AU it is reasonable to choose $V_{max} - V_{min} \gtrsim 100$ km/sec. which is approximately twice the magneto-acoustic speed, V_m. The decline is a monotonic decrease in V from V_{max} to a value near V_{min}, lasting 2-7 days. Examples of simple streams are marked "S" in Figure 1. Obviously, even simple streams can display different characteristics. This will be discussed later, but a further morphological classification is not very fruitful at this point.

Compound Streams - are similar to simple streams, but either the rise or the decline is interrupted by a substantial increase in V. If this occurs during the rise, one observes a change in slope of the rate of increase in V. Examples of such streams are marked "C" in Figure 1.

Irregular Variations (substreams) - These are characterized by changes in V which are less than the magnetoacoustic speed and which lasts less than a day or two. Some examples are denoted by "I" in Figure 1.

This classification is not unambiguous, because there is actually a spectrum of variations. On the other hand, one can identify some physically distinct flows corresponding to each of the classes listed above. For streams, $\Delta V \equiv V_{max} - V_{min} > V_m$ implies that the change in the kinetic energy density across the "rise" $\Delta(\rho \frac{V^2}{2})$, is greater than the total pressure $\frac{B^2}{8\pi} + nkT$, whereas for irregular variations this is not so. Thus, the pressure gradient might significantly alter the speed profile of an irregular variation as time goes on, whereas the opposite is the case for streams with $\Delta V \gg V_m$. Irregular variations will not be discussed in this review, although they obviously merit further investigation.

Simple streams are presumably generated by some perturbation near the Sun. A compound stream appears to be the result of a faster stream overtaking a slower stream and is presumably due to two successive (adjacent) perturbations near the Sun. In general, the source function is probably not a succession of isolated pulses, but rather an irregular function which reflects the complexity of the solar corona. Nevertheless, it is convenient to begin by considering models of simple streams, which illustrate the basic physical processes. Later, one can consider the

the effects of the interactions among streams, which produce compound streams. Ultimately, one might construct models for very general, time varying source functions to describe variations over a period of many days, but no attempt to do so will be made here.

Physically, it is desirable to distinguish between streams on the basis of their origin. This brings us back to the ideas mentioned in the introduction, which arose in studies of geomagnetism. We shall distinguish two types of simple streams: flare-associated streams and "corotating" streams (which need not be stationary). This distinction has been questioned by Ballif and Jones (1969), but the results which follow support the concept of two kinds of streams.

3.0 Corotating Streams

3.1 Structure and Dynamics - Figure 2 illustrates schematically some of the important structural and dynamical features of a corotating simple stream. The stream connects to a region on the Sun (M-region?) which acts as a continuous source of material. It has a spiral geometry because the material moves nearly radially at a constant speed while the source rotates with the Sun, as discussed, e.g., by Chapman (1964). There is a region in which the pressure is high (the interaction region), that occurs generally in the rising part of the speed profile, but extends somewhat ahead of the point where V begins to increase and somewhat behind V_{max}. (Burlaga and Ogilvie, 1970; Siscoe, 1972; Ogilvie and Burlaga, 1974). In the interaction region, the density, temperature, and magnetic field intensity reach relatively high values. The region of enhanced density (compression region) is displaced ahead of the enhanced temperature region (hot spot) (Burlaga et al., 1971), and at 1 AU these two regions are separated by a thin boundary called the stream interface (Burlaga, 1974). Ahead of the interface, ambient material that has been swept up by the stream is deflected to the West, while stream material behind the interface slips to the East. In the region behind V_{max}, the density and temperature are relatively low (e.g., Gosling et al., 1972; Burlaga and Ogilvie (1970); Burlaga et al., 1971; Siscoe, 1972), and accordingly it is referred to as the rarefaction region. Beyond 1 AU a shock pair is presumed to form as the pressure pulse in the interaction region increases in amplitude.

Most of the general features just described can be seen in the examples of some actual streams shown in Figures 3 and 4. Figure 3 shows an interaction region observed by Explorer 43. One can see the elevated pressure, $P = \frac{B^2}{8\pi} + nk\,(T_p + T_e)$ (with the unmeasured T_e set equal to $1.5 \times 10^{5\circ}$) concentrated in the region where V is increasing. The high density region ahead of the high temperature region and the interface which separates them are also evident. The magnetic field intensity is high in the interaction region, and generally one finds that the peak of B follows the peak in n by a few hours (Davis et al., 1966; Burlaga et al., 1971; Ness et al., 1971) as in this case. The magnetic field direction usually fluctuates considerably in the interaction region (Burlaga et al., 1971).

Figure 4, which is based on hourly averages, shows some of the features just mentioned and two additional features of corotating streams: 1) in the part of the interaction region ahead of the interface (indicated by the vertical lines), the flow is from several degrees East, consistent with the Westward deflection mentioned above, and in the interaction region behind the interface the flow is several degrees from the West of the Earth-Sun line; 2) in the region of declining V, ρ falls to very low values which are below the pre-stream values, corresponding to the rarefaction that was mentioned. No systematic North-South deflection is shown in this case, but such variations occassionally do occur (Sullivan and Siscoe, 1974).

No single model reproduces all of the effects described above. The approach has been to construct simple models to explain individual effects.

Some of these models will now be briefly reviewed.

Parker (1962) was the first to point out that high speeds could be obtained by raising the temperature at a heliocentric distance of several solar radii. Burlaga and Ogilvie (1970) found experimental support for this type of mechanism. Burlaga et al. (1971) showed that a stream with many of the observed characteristics could be obtained by raising the temperature at 0.1 AU at a constant rate, from $6 \times 10^{5\circ}$K to 7×10^{6} $^{\circ}$K in 60 hrs., and then reducing it linearly to the original value. The results obtained in this way are shown in Figure 5. This calculation was based on a spherically symmetric, time-dependent, one-fluid computer code that Hundhausen and Gentry (1969) developed for shocks. The energy equation was replaced by the adiabatic relation $P = A(s)\,\rho^{\gamma}$, where the entropy, s, of a given volume element is a constant, but different volume elements have different entropies. The electrons were not treated explicitly, but it was argued that their thermodynamic properties could be treated separately, as will be discussed later. It was argued that the use of spherical symmetry to describe some of the features of corotating streams is justified because the basic dynamical effects are the result of radial pressure gradients caused by the kinematic steepening of the streams; a formal justification for this procedure was recently given by Hundhausen (1973a). Summarizing, the high speeds, the asymmetrical speed profile, the high density, and high temperature regions, and the displacement of these two regions are accounted for by postulating that streams are the result of a time varying temperature at $\approx$ 0.1 AU. The time variation of the source temperature are primarily due to corotation of a hot region past the sub-solar point.

The results presented in Figure 5 do not show an interface; on the other hand, a rather weak stream was considered, the speeds ranging from 275 km/sec to 400 km/sec. Recent calculations (Hundhausen and Burlaga, 1974) with somewhat larger perturbations in T at 0.1 AU, which give changes of V from 325 km/sec to 475 km/sec., show that an interface does indeed form near 1 AU according to the model just described. Pure density perturbations or pure speed perturbation, do <u>not</u> give rise to an interface. Thus, the interface represents a signature of the source mechanism. Lewis and Siscoe (1972) showed analytically, in a <u>linear</u> approximation, that a temperature perturbation near the Sun, rather than a density or speed variation, is needed to explain the kinds of density and speed variations observed at 1 AU, but their model does not produce an interface.

The East-West deflections described above obviously cannot be explained by a model which imposes spherical symmetry. Intuitively, the reason for the deflection is clear, and it has been long recognized that such a flow pattern should be observed. Several models have been published which account for the E-W deflections. These are steady-state, corotating stream models in which streams are presumed to exist at .1 AU with a symmetrical speed profile and no density or temperature perturbations. Linear models were presented by Siscoe and Finley, 1972, among others. A non-linear model was first published by Goldstein (1971). These models do not account for the separation between the dense region and the hot region, because of the assumption of no source temperature perturbation.

3.2 Magnetic Fields

The variation of the magnetic field through streams has been the subject of several theoretical studies, (e.g., Goldstein, 1973; Urch, 1972; and Matsuda and Sakurai, 1972). These concentrate on the configuration of the field, rather than the intensity. No evidence of a systematic variation of the direction of $\underset{\sim}{B}$ through streams has been published, but it is clear that if such a variation exists, it is much smaller than the fluctuations that are seen on a scale of several hours. In the author's opinion, it is more important to explain the intensity-time profile. The relevant observations are not yet completely analyzed, but it is clear from what has been said earlier that a) the field intensity is highest in the interaction region; b) the maximum of B generally follows that of n by a few hours.

Qualitatively, the high magnetic field intensities in the interaction regions are readily understood as the result of the compression in the rising portion of the stream. Since the magnetic field is "frozen" to the plasma, one expects B to be generally high when n is high.

The observed displacement between B and n might seem to contradict the "frozen-in" condition, but the equation relating $\underset{\sim}{B}$ and ρ is

$$\frac{D}{Dt}\left(\frac{\underset{\sim}{B}}{\rho}\right) = \left(\frac{\underset{\sim}{B}}{\rho} \cdot \nabla\right) \underset{\sim}{V},$$

indicating that $B \sim \rho$ only if V is constant. When $\underset{\sim}{V}$ is radial, for example, $\frac{D}{Dt}(\underset{\sim}{B}/\rho) = \left(\frac{B}{\rho}\right)\frac{\partial V}{\partial \Omega}$, which says that the ratio $\underset{\sim}{B}/\rho$ in a volume element decreases in the rising part of a stream, where $\frac{\partial V}{\partial \Omega} < 0$. Perhaps an additional contribution to the separation between the high B and high n regions lies in conditions at the inner boundary. If distinct volume elements have different B/ρ values, these differences will be conserved even if B/ρ remains constant for each volume element along its trajectory. This possibility has been suggested by Richter (private communication).

The variation of magnetic fluctuations through streams is of considerable importance to geomagnetism, but relatively little is known about this. Generally, the fluctuations are high when the speed is high (Davis et al., 1966; Belcher et al., 1969; Hirshberg and Colburn, 1969; Sari, 1972). The most intense fluctuations occur in the interaction region (Davis et al., 1966; Coleman, 1968) and seem to be confined to this region (Burlaga et al., 1971). The fluctuations in the interaction region have been attributed to the Kelvin-Helmholz instability (Coleman, 1966), but Burlaga and Ogilvie (1970) argued that this instability is not an important mesoscale process at 1 AU. It is likely that the fluctuations in the interaction region are due to an interplanetary process associated with the steepening of a stream, but the process has not been identified. The other fluctuations, which seem to depend on V, have been studied by Belcher et al., (1969) who identified them as Alfvén waves; but their origin is also not understood. The subject of fluctuations is already a very large one, and our remarks do little more than identify it. The review presented by Völk at this meeting discusses the subject more throughly. Much more remains to be done. We stress the importance of considering fluctuations in relation to the different types of stream profiles.

3.3 Thermal Structure (Protons)

Figure 6 from Burlaga and Ogilvie (1973) shows the variation of T and V for a few streams. The temperature rises rapidly with V to a maximum in the interaction region ahead of V_{max}, and then returns to the original value with lower temperature at a given V during the "decline" than during the "rise".

Burlaga and Ogilvie (1973) showed that the variation of T at streams could approximately be represented by the sum of two components, $T(t) = T(V(t)) + \Delta T(t)$; where $\sqrt{T(V)} = a\ V + b$ is a relation between T and V which is valid on a scale of several solar rotations (Burlaga and Ogilvie, 1970; Hundhausen et al., 1970) (See Figure 7). This T-V relation is independent of solar cycle (Figure 7) and is probably a consequence of the way that streams are generated, e.g., by raising the temperature near the Sun (Burlaga and Ogilvie, 1971 and 1973) as discussed earlier. Pizzo et al. (1973) and Hundhausen (1972b) expressed some reservations about this interpretation, but Hundhausen (1973a) concluded that the T-V relation is basically a consequence of the acceleration mechanism, in general agreement with Burlaga and Ogilvie.

The component $\Delta T(t)$ above is, according to Burlaga and Ogilvie (1973), of interplanetary origin, being positive in the region of increasing V due to compression, and negative in the region of decreasing V due to expansion, (see Figure 6, where $T - T_c \equiv \Delta T$). In the models of Burlaga et al. (1971), Hundhausen (1973a), and others, the compression is assumed to be approximately adiabatic. This has been criticized on the ground that it does not show how the protons are heated in the interaction region, (e.g., Papadopoulos, 1973), since it substitutes an adiabatic law for the energy equation. Of course, this criticism is partly justified, since one would like to know the actual heating mechaniam, but it does not follow that the existence of such a mechanism invalidates the fluid approximation, which actually gives a good description of the mesoscale configuration of streams.

The search for a heating mechanism in the interaction region is basically a search for an appropriate plasma instability. Goldstein and Eviatar (1973) suggested that energy is transferred by an electromagnetic two-stream instability. However, enhanced magnetic field fluctuations near the proton gyrofrequency are not generally observed in interaction regions, (Goldstein, private communication). Papadopoulos et al. (1974) considered that the electrostatic ion-ion, 2-stream instability is the dominant one. Both they and Goldstein and Eviatar (1973) assume that initially the velocity profile is a step function whose edge is eroded with time. Such a microscopic model cannot, of course, explain the origin of high speed streams. A hybrid fluid-kinetic model, such as that of Papadopoulos et al. (1974), should explain the observed stream structure, including the T-V relation. The T-V relation did not appear in the results of Papadopoulos et al. (1974), perhaps because of an inappropriate choice of initial conditions.

4.0 Flare-Associated Streams

4.1 Structure and Dynamics

Less is known about flare-associated streams than corotating streams, because they are infrequent, complex, and inherently transient. In practice, such streams have been identified by looking for a shock preceeding a stream and a large (type 2 or 3) flare occurring a few days prior to the arrival of the shock at 1 AU. Most of the studies to date have been based on examining only one parameter (e.g. $\underset{\sim}{B}$, T_p, T_e, n_α/n_p) for several events, rather than comprehensive studies of individual events. A synoptic picture, constructed by Hundhausen (1972b) from these studies is shown in Figure 8. The arrival of the stream is presumed to be marked by a tangential discontinuity, (which has not often been unambiguously identified) followed by a shell of material with an anamalously high He^{++} abundance. The highest speeds occur behind the He^{++} shell, and it has been suggested, (but not demonstrated conclusively), that the magnetic field has a bottle or loop-configuration in the fast stream. The stream originates in the site of a flare and drives a shock ahead of it, as shown in Figure 8.

One of the best examples of a flare-associated stream is the February 15, 1967 event. This originated in a Type 3 flare at 10°W at 1815 UT on February 13, 1967. A shock arrived at Earth at 2348 UT on February 15. The n, V, B profiles for this event are shown in Figure 9, from Arnoldy (1971) together with 2 other parameters that will be discussed later. One sees a rather steep stream, and a high density and magnetic field intensity in the interaction region, due both to the shock and the steepening of the stream. According to Hirshberg et al. (1970) material with a very high He^{++}/H^{+} ratio passed the Earth beginning $\approx$ 0915 UT on February 16, and presumably marks the arrival of material ejected from the flare site.

At the time that the February 15, 1967 event was observed at Earth, Pioneer 7 was monitoring the solar wind at 1 AU, 25° East of the Earth-Sun line. The stream profile shown in Figure 9 was not seen earlier by Pioneer 7, i.e. the stream was not corotating. Instead, another, much broader stream, was observed. Scudder and Burlaga (1974) inferred that the spatial configuration was as illustrated in Figure 10. Because the stream originated in the flare-site at 10° West, and because its angular half-width was less than 35°, it was not detected at Pioneer 7. However, there was a corotating stream in the vicinity of this flow, and the flare associated flow interacted with it. In particular, the shock driven by the flare-associated stream was decelerated in the high-density region ahead of the corotating stream, producing the distortion illustrated in Figure 10. This process was analyzed by Scudder and Burlaga (1974) for a shock of arbitrary strength in the non-linear limit and by Heineman and Siscoe (1974) for a set of strong shocks in a linear model. An important point here is that the shock has a much greater angular extent than the stream, and may consequently interact with other streams, so that the flow behind some parts of a flare-associated shock may not be the flare-associated stream. This was discussed also by Ogilvie and Burlaga (1974).

4.2 Composition

Anamalously high He^{++} abundances behind some shocks have already been mentioned. The most extensive study is that of Hirshberg et al. (1972) who found high He^{++} abundances ($n(He^{++})/n(H^{+})$ ranging from $\sim$0.15 to 0.3) 5 to 15 hrs. behind several shocks that were associated with Type 2 or Type 3 flares. The width of the He-rich region ranges from $\sim$0.1 to 0.3 AU. The angular extent of the He-enhancements with respect to the flare sites is large—from 65° West to 42° East in the study of Hirshberg et al. (1972). This is presumably a measure of the angular width of flare-associated streams. The results are consistent with the early inference from geomagnetic and solar observations made by Newton (1943), that the width of such streams is typically $\pm$ 45°.

Figure 11, from Montgomery (1974), illustrates the variation of helium abundance (alpha fraction) for one event. Note the abrupt increase approximately 12 hours after the shock. This is what has been identified as the piston boundary. The reason for the high He^{++} abundance behind some shocks is not known with certainty. However, Ogilvie et al. (1968) and Hirshberg (1968) suggested that the material containing this helium was ejected by the flare from a region low in the corona, where the abundance of He^{++} may be higher because of gravitational separation.

4.3 Thermal Structure and Magnetic Fields

Perhaps the most important recent work on flare-associated streams concerns the temperatures of protons and electrons. Montgomery et al. (1974) found that there is a very strong tendency for unusually low electron and proton temperatures to follow interplanetary shock waves by 10-20 hrs. and remain low for 25-70 hrs. In particular, they found 13 such cool regions in the period August, 1967 to May, 1971, and 12 of these were preceded by shocks or SSC's. One case is shown in Figure 11. Similarly, Gosling et al. (1973) found that regions in which T_p was anamalously low followed shocks or SSC's by 20-60 hrs. Many of the cool regions are also preceded by abnormally high concentrations of helium.

In Figure 11, the speed profile itself is not very impressive, $V_{max} - V_{min}$ being only $\approx$ 100 km/sec, but the structure in the other parameters is most interesting. The shock is clearly seen at $\approx$ 0600 UT on May 17. It is followed by a high density, high temperature region and a possible interface at $\approx$ 0900 UT on May 17. Near V_{max}, however, there is an abrupt drop in N, T_p, and T_e, and an enhancement of the α concentration, suggesting that this is a piston boundary as envisaged by Hirshberg et al. (1970). Behind this boundary, both T_p and T_e are very <u>low</u>, despite the relatively high speeds. This is difficult to explain on the basis of the corotating stream model discussed earlier, because it implies that T should be <u>high</u> when V is high.

Both Montgomery et al. (1974) and Gosling et al. (1973) suggested that the low temperatures are the consequence of cooling in an expanding magnetic bottle or loops. The lower heat flux observed in the cool zone (Montgomery et al., 1974) supports this view, and suggests that the loops are closed as a result of reconnection. However, other hypotheses cannot be excluded; for example, the cooling could simply be the result of expansion of material ejected under a high pressure from a very small region near the flare site. Mathematical models of this process are needed. Obviously, one can hope to hearn more about heat conduction and the thermal coupling between protons and electrons in a collisionless plasma from such studies.

Additional indirect evidence for magnetic bottles was presented by Barnden (1973) who observed that some Forbush decreases procede in 2-steps, the first following a shock and the second following what he considers to be the piston boundary behind which is a magnetic bottle that excludes cosmic rays. The configuration which he infers from such events is shown in Figure 12.

Little has been published concerning the direct measurements of the magnetic fields in the cool regions behind shocks, although such results will be forthcoming within a year. Schatten and Schatten (1972) have studied this problem and concluded that interplanetary fields were compressed behind the shocks, but loops were not observed. Actually, their results do not exclude loops, but require that, if loops occur, the field in them is not high.

5.0 Interaction of Streams with Earth

5.1 Introduction

Space restrictions do not allow a review of work on all aspects of the interaction of the solar wind with the Earth. There is an extensive literature on the subject, largely based on correlations between pairs of parameters which are aimed at finding the most important factors that cause geomagnetic activity. Because of the large number of interplanetary parameters available and the several geomagnetic indices, there are many possible combinations which have been explored. Two factors seem to be particularly important: 1) a sufficiently large Southward component of $\underset{\sim}{B}$ (B_z) (e.g. Dungey, 1961; Fairfield and Cahill, 1966; Kane, 1972 and 1974; Hirshberg and Colburn, 1969), and 2) fluctuations in $\underset{\sim}{B}$ (e.g. Coleman et al., 1966; Garret, 1973; Jones et al., 1974). Other correlations have been reported and debated, such as the relation between K_p and V. It is becoming recognized that no single factor determines geomagnetic activity, and consequently further 2-parameter correlations will probably not be very fruitful.

Another approach, which is closer to the historical one, is being developed and is providing new insights, namely, the consideration of the relations between interplanetary streams and geomagnetic activity. This promises to be the key link between interplanetary dynamics and the dynamics of the solar wind-Earth interaction.

Whereas the historical approach began with geomagnetic effects and sought to explain their causes in terms of streams, the availability of in situ measurements allows us to examine both the causes of geomagnetic disturbances and the effects of interplanetary streams. The following discussion examines some of these relations that have been identified recently.

5.2 General Effects of Streams on Geomagnetic Activity

Snyder et al. (1963) reported a strong correlation between V and the three-hour geomagnetic index, K_p, and they related periods of geomagnetic activity to interplanetary streams. They concluded that the streams recurred on several successive solar rotations, and hence identified them as corotating streams originating in M regions on the Sun. Only two of the streams caused sudden commencements.

These early results were not fully confirmed by subsequent studies, although the differences are largely a matter of degree. For example, Gosling et al. (1972b) showed that the persistence of streams is not as great as Snyder et al. originally suggested, since the correlation of speeds at a 27 day lag was only 0.4 for the Mariner 2 data in 1962. This can actually be seen by inspection of the velocity profiles in the paper of Snyder et al., (even though the eye tends to see a higher correlation). Similarly, a close look at Figure 13 shows that K_p is not always directly proportional to V, but rather that there are cases where K_p is largest when V is increasing. We shall consider these effects more closely later, in relation to individual streams.

Figure 1 from the Solar Terrestrial Chart STAC-A for 1968, shows the horizontal component of the geomagnetic field and the A_p index together with the speed profile, which is divided into streams as discussed in Section 2. Once again, note that the stream profiles are generally more complicated than the simple flows' discussed in the previous two sections, due to interactions among the various types of streams and the "irregular" flows. Some streams are preceded by SSC's, indicated by the solid triangles, in Figure 1, and may be flare-associated. However, most streams are not preceded by SSC's, consistent with the general result of Snyder et al. (1963) and others that most streams are "corotating" rather than flare-associated. Conversely, most SSC's do not occur ahead of streams, which is consistent with our earlier discussion of how a shock can move through a stream of independent origin. Even if every shock were driven by a flare-associated stream, one would expect to see the driver-stream only for a narrow range of longitudes relative to the flare, corresponding to the relatively narrow width of the stream, while the shock extends over a much greater range of longitudes where it may be associated with some other stream.

The largest geomagnetic effects during the first half of 1968, indicated in Figure 1 by large depressions in the H component of the Earth's magnetic field and high A_p indices (shaded areas in Figure 1), follow interplanetary shock fronts (indicated by SSC). Five cases are shown: one shock is followed by a large stream; one is followed by a small stream; one is not accompanied by a stream; and for two there is no plasma data. Thus, not all SSC events are caused by flare-associated streams, but apparently some are caused by such streams.

The corotating streams in Figure 1 (which we assume are those that are not preceded by sh ks) generally cause a depression in H and are usually associated h A_p, but this is not always so. The geomagnetic effects of these streams are smaller than those associated with shocks.

Let us now consider the geomagnetic effects of some specific streams. Figure 14 from Bobrov (1973) shows two different kinds of streams and two corresponding types of geomagnetic disturbances. The October 1962 disturbance was caused by a large stream which is one of those that Snyder et al. (1963) observed to recur and which was not preceded by a shock or SSC; i.e., it is a corotating stream. The April, 1968 disturbance in Figure 14 was caused by a non-recurring stream which was preceded by a shock, and was presumably flare-associated. The speed, density, and magnetic field intensity profiles are similar for the two events; i.e., regardless of the origin, the streams steepen kinematically as they move away from the Sun with the consequent compression of n and B in the region of increasing V. But the geometries of the streams probably differ, and there may be other physical differences as well. Most interesting is the observation of Bobrov that the geomagnetic effects of the two streams were rather different, in that K_p remained high nearly <u>throughout</u> the passage of the corotating stream whereas K_p was confined only to the passage of the interaction region of the flare-associated stream.

Bobrov (1973) suggests that geomagnetic activity is high during the passage the interaction regions of both corotating and flare-associated streams because both negative B_z and the fluctuations in $\underset{\sim}{B}$ are high in the interaction regions. He shows that the high K_p in the trailing part of corotating streams is due to the presence of large fluctuations in $\underset{\sim}{B}$

there. It would be interesting to investigate whether the absence of fluctuations in the trailing part of flare-associated streams is associated with magnetic loops or bottles.

The February 15-22, 1967, event, (Figure 9) which was discussed in Section 4 is a flare-associated stream. Arnoldy (1971) has examined the relation between this stream and the AE index, concluding that AE is correlated (0.8 correlation coefficient) with the time-integral over B_z South for the hour preceding the AE hourly average (B T in Figure 9). Thus, in this event, merging is apparently the most important process in producing geomagnetic activity (at least in the auroral zone). Hirshberg and Colburn (1969) showed that in this event the fluctuations in $\mathbf{B}$ disappeared abruptly several hours after the passage of the presumed piston boundary.

5.3 Geomagnetic Impulses

This subject was reviewed by the author at the last STP meeting (Burlaga, 1972). Here, only some work that appeared since 1970 is discussed.

There have been many attempts to establish the causes of SSC's (see the reviews by Burlaga, 1972 and Hundhausen, 1972b). The most comprehensive study was published by Chao and Lepping (1974) who considered 93 SSC's in the period January 1968—June 1971. They found that 87% of the SSC's were related to solar events. Interplanetary measurements were available for 48 of those SSC's and it was found that 85% were caused by shocks, the remaining 15% being due to tangential discontinuities. Fifty percent of these shocks were related to Type 2 or Type 3 flares, suggesting that perhaps most (but not necessarily all) interplanetary shocks are related to flare-associated streams. However, the problem of flare-association is a difficult one and has not been solved. It is important to examine the flows behind shock waves which are observed within $\pm$ 30° of the lines between the observer and the sites of the flares which produce such shocks.

Recently, Ogilvie and Burlaga (1974) identified two extreme types of interplanetary, post-shock flows. In one case, only one discontinuity followed the shock front; in the other case, at least 14 discontinuities were observed within 24 hours after the shock. Similar flows were discussed by others (e.g., Burlaga, 1972 and Hundhausen, 1972b). The two types of flow patterns can be recognized in magnetograms, as shown in Figure 15. In the one case the H component varied relatively smoothly behind the SSC, whereas in the other case, many sudden impulses were observed, corresponding to the change in momentum flux across each of the interplanetary discontinuities.

The existence of geomagnetic events characterized by a SSC followed by many impulses was noted by Yoshida and Akasofu (1966), and considered in more detail by Moldovanu (1973) and Moldovanu and Brandu (1973), who labeled them gr(SC + SI) events. The occurrance of such events for rotations 1839-1845 (December 1967 to June 1968) is illustrated in Figure 16, from Moldovanu; the solid triangles indicate SSC's and the open triangles indicate sudden impulses. Moldovanu argued that gr(SC + SI)s occur at corotating streams, near sector boundaries. Inspection of Figure 16 shows that none of the gr(SC + SI) events recurred on two successive rotations, and some occurred near sector boundaries whereas others did not. The occasional association of shocks with sector boundaries may, however, have a physical basis, and further studies are warranted.

To explain the cause of gr(SC + SI)'s, Moldovanu adopts the model of Dessler and Fejer (1966) in which a shock pair and an unstable tangential discontinuity are presumed to exist ahead of a stream at 1 AU. However, neither his data nor in-situ measurements of streams show the existence of shock pairs at 1 AU (e.g., Ogilvie, 1972). The process which Dessler and Fejer proposed probably does occur just beyond 1 AU, and the tangential discontinuity in their model is possibly observed at 1 AU as the stream interface (Burlaga, 1974). The in-situ observations suggest that this discontinuity is stable at 1 AU, and no geomagnetic effects were found to be associated with it.

5.4 Time Variations of Streams and Geomagnetic Activity

If geomagnetic activity is strongly related to interplanetary streams, then one should find that temporal variations in streams should cause corresponding changes in geomagnetic activity. This is confirmed by the results of several studies that are reviewed below.

Gosling et al. (1972b) showed that at solar minimum the stream structure had a 27 day periodicity, but they emphasized that the streams were not stationary, the peak correlation of V near a lag of 27 days being only 0.4-0.5. This is illustrated in Figure 17, which shows the autocorrelation function of V for July 7 to November 6, 1964. There is a tendency for streams to persist for more than one solar rotation, but streams seldom persist for more than two solar rotations, and many streams do not persist for even one solar rotation. Thus, even at solar minimum, the streams are evolving.

Gosling et al. (1972b) suggested that the evolution of stream patterns changed with solar activity, and they showed that the auto-correlation coefficient was only ≈ 0.3 in the period 1962-1967. Intrilligator (1974) proposed that the number of streams varies with solar activity. Because of the importance of this question, her analysis should be confirmed. The data set used by Intrilligator contained numerous gaps and some quick-look data which is erroneous); and she did not rigorously distinguish between the different kinds of speed variations. Montgomery et al. (1972) reported that the number of large-scale disturbances during the period 1963-1969 remained constant (a few per 27-day interval), with the most energetic events occurring only near solar maximum.

The results just described only suggest the kind of long-term relations that exist between interplanetary streams. They could best be studied by long-term, simultaneous measurements of both geomagnetic and interplanetary activity. At the moment, however, the interplanetary data and geomagnetic observations are complementary, the latter providing a continuous record and the former providing information which is needed to interpret this record.

Assuming that relations exist between streams and geomagnetic activity, one can use the long-term geomagnetic observations to study the long-term variations of streams. Abdel-Wahab and Goned (1974) computed power spectra of K_p for the 1932-1969 period. They found a clear variation with solar cycle, a 27-day periodicity being predominant at solar minimum and much less pronounced at solar maximum (Figure 18). At solar minimum, they observed peaks at 1/27 $(\text{day})^{-1}$ and 1/13.5 $(\text{day})^{-1}$, presumably corresponding to the streams in the sectors observed by Wilcox and Ness, (1965) and Ness and Wilcox, (1966), and they also found peaks at 1/9, 1/7 and 1/5 $(\text{day})^{-1}$ corresponding to the particular pattern of streams. Near solar maximum the higher frequencies are not well-defined, and the amplitudes of the 1/27 and 1/13.5 $(\text{day})^{-1}$ peaks are much smaller than at solar minimum. Evidently, as solar activity increases, the stream structure becomes more complex, perhaps because of the evolution of individual corotating streams or the random injection of additional, flare-associated streams.

Summary

A complex chain of events relates geomagnetic activity to solar activity, and interplanetary streams are a key link in the chain. This was obscured by the many correlative studies between interplanetary and geomagnetic time series, but in recent work there is a return to the earliest approach which emphasized streams. We have shown, for example, that two of the factors which influence geomagnetic activity, the southward component of the interplanetary magnetic field and the fluctuations in the magnetic field, are related to stream profiles, and are presumably a consequence of interplanetary stream dynamics.

There is a variety of speed profiles, but two classes are particularly important—corotating streams and flare-associated streams. These can interact with one another in complicated ways producing compound streams and other complicated configurations.

Many features of corotating streams (e.g., the compression and rarefaction, the stream interface, the separation between the density and magnetic field peaks, the East-West deflection, and the temperature speed relations) can be explained by a model which postulates that streams are the consequence of a hot, corotating region in the solar envelope. The processes associated with heat conduction and waves are still not fully understood and are being studied. Much also remains to be learned about the causes of the magnetic fluctuations and their relations to streams.

Less is known about the dynamics of flare-associated streams. For example, there is some indirect evidence of magnetic loops in the flare ejecta and a suggestion that the field is relatively uniform in those loops, with a consequence that they do not produce much geomagnetic activity; but little is known with certainty. Some shock fronts are followed by numerous discontinuities, and are observed in magnetograms as "gr(SC + SI) events". The cause of such flow patterns remains to be determined, and the possible relation to the magnetic sector structure needs to be examined further. Flare-associated streams are less frequent than corotating streams but they generally produce greater geomagnetic disturbances and are intrinsically transient. Corotating streams are more persistent, but they too evolve on a scale of one solar rotation. There is a change in the stream configuration with solar activity, but it is not understood whether this is due to a change in the <u>number</u> of corotating and/or flare-associated streams or some other cause.

Clearly, much remains to be learned about the solar wind-Earth interaction, but the return to the early concept of streams interacting with the Earth offers a fresh approach to the study of the dynamical sequence of events relating the origin and development of streams to geomagnetic activity.

Acknowledgements

The author thanks Drs. L. Barouch, D. Fairfield, and K. Ogilvie for their very helpful comments on a draft of this paper.

Figure Captions

Fig. 1 Interplanetary streams and geomagnetic activity. The speed and density profiles are divided according to the three classes described in the text. Most streams have some influence on the A_p index or H component of the Earth's field, but the largest disturbances follow sudden commencements, caused by shocks, which are indicated by the solid triangles.

Fig. 2 A schematic illustration of the basic features of a corotating stream.

Fig. 3 Stream interaction region. The pressure is high in the region where V is increasing. The region of high density is separated from that of high temperature by a thin boundary called the stream interface, and the highest magnetic field intensities follow the high densities.

Fig. 4 A corotating stream. Note the separation between the peak density and peak magnetic field, the density rarefaction, and the East West (EW) deflection.

Fig. 5 A model of a stream generated by a temperature perturbation.

Fig. 6 Temperature and speed profiles for several streams. $T-T_c$ is the measured temperature minus that which is predicted by the T-V relation and approximately represents the change in T due to interplanetary dynamical processes.

Fig. 7 Temperature-speed relations (dashed lines) for March 18-April 8, 1971 (Explorer 43), June-December, 1967 (Explorer 34) and December, 1965-May, 1966 (Pioneer 6). There is essentially no change with solar activity. The effects of interplanetary heating are small, as indicated by the small separation between the T-V relation for intervals of increasing speed ($\Delta V>0$) and that for intervals of decreasing speed ($\Delta V<0$).

Fig. 8 A synoptic view of flare-associated stream features.

Fig. 9 Speed, density, and magnetic field profiles for a flare-associated stream, together with the AE index and an average of the South-B_Z component of the interplanetary magnetic field. This flow configuration and the strong relation between ΣB_Z T and AE are typical of such streams.

Fig. 10 Schematic view of the flow associated with the February 15, 1967 event. Note that the flare-associated stream interacted with a corotating stream and the shock was modified by the interaction region of the corotating stream.

Fig. 11 Flow pattern for a flare-associated stream. Note the low temperature near the maximum speed.

Fig. 12 The magnetic field configuration in flare-associated streams, inferred from cosmic ray observations. The shading indicates the extent of the depletion of cosmic rays. The dashed lines show the shock and piston-boundary.

Fig. 13 Relation between K_p and V. There is a general correlation, but occasionally K_p is largest in the interaction region, where V is increasing.

Fig. 14 A corotating stream (a) and a flare-associated stream (b). Although the n, V, B profiles are similar, indicating similar dynamic development, the geomagnetic effects are very different, perhaps because of different magnetic field configurations.

Fig. 15 Momentum flux behind two interplanetary shock fronts and the H component of Earth's magnetic field measured at Honolulu.

Fig. 16 Geomagnetic impulses and sector pattern, December - June, 1967.

Fig. 17 Autocorrelation of the interplanetary speed profile, illustrating that streams tend to recur only once or twice.

Fig. 18 The intensity of the 1/27 $(\text{day})^{-1}$ peak in the power spectrum of K_p for various parts of the solar cycle. Recurring streams are most prominant near solar minimum, and the recurrence tendency is weak at solar maximum.

References

Abdel-Wahab, S., and A. Goned, Planet Space Sci., 22, 537, 1974.

Akasofu, S., and S. Chapman, Solar-Terrestrial Physics, Oxford University Press, London, 1972.

Arnoldy, E. L., J. Geophys. Res., 76, 5189, 1971.

Ballif, J. R., and D. E. Jones, J. Geophys. Res., 74, 3499, 1969,

Barnden, L. R., Proc. 13th International Cosmic Ray Conference, Vol. 2, p. 1277, 1973.

Bartels, J., Terr. Magn. Atmos. Elect., 37, 1, 1932.

Belcher, J. W., L. Davis, and E. J. Smith, J. Geophys. Res., 74, 2302, 1969.

Bobrov, M. S., Planet. Space Sci., 21, 2139, 1973

Burlaga, L. F., Solar Terrestrial Physics; Part II, p. 135, D. Reidel Publishing Company, Dordrecht-Holland, 1972.

Burlaga, L. F., J. Geophys. Res., in press, 1974

Burlaga, L. F., and K. W. Ogilvie, Astrophys. J., 159, 659, 1970.

Burlaga, L. F. and K. W. Ogilvie, J. Geophys. Res., 78, 2028, 1973.

Burlaga, L. F., K. W. Ogilvie, D. H. Fairfield, M. D. Montgomery, and S. J. Bame, Astrophys. J., 164, 137, 1971

Chao, J. K., and R. P. Lepping, J. Geophys. Res., 79, 1799, 1974.

Chapman, S., Solar Plasma, Geomagnetism, and Aurora, Gordon and Breach, New York, 1964.

Coleman, P. J., Jr., Astrophys. J., 153, 371, 1968.

Coleman, P. J., Jr., L. Davis, Jr., E. J. Smith, and D. E. Jones, J. Geophys. Res., 71, 2831, 1966.

Davis, L., E. J. Smith, P. J. Coleman, and C. P. Sonett, in The Solar Wind, p. 35, ed. R. J. Mackin, Jr., and Marcia Neugebauer (New York: Pergamin Press), 1966.

Dessler, A. J., and J. A. Fejer, Planet. Space Sci., 11, 505, 1963.

Dungey, J. W., Phys. Rev. Lett., 6, 47, 1961.

Fairfield, D. H., and L. J. Cahill, J. Geophys. Res., 71, 155, 1966.

Gold, T., J. Geophys. Res., 64, 1665, 1959.

Goldstein, B., Analysis of fluctuations in the solar wind, Massachusetts Institute of Technology, Ph.D. Thesis, 1971.

Goldstein, B. E., Eos, 54, 1190, 1973.

Goldstein, M., and A. Evitar, Astrophys. J., 179, 627, 1973.

Gosling, J. T., R. T. Hansen, and S. J. Bame, J. Geophys. Res., 76, 1811, 1971.

Gosling, J. T., A. J. Hundhausen, V. Pizzo, and J. R. Asbridge, J. Geophys. Res., 77, 5442, 1972.

Gosling, J. T., V. Pizzo, M. Neugebauer, and C. W. Snyder, J. Geophys. Res., 77, 2744, 1972b.

Gosling, J. T., and S. J. Bame, J. Geophys. Res., 77, 12, 1972.

Gosling, J. T., V. Pizzo, and S. J. Bame, J. Geophys. Res., 78, 2001, 1973.

Heinemen, M. A., and G. L. Siscoe, J. Geophys. Res., 79, 1349, 1974.

Hirshberg, J., Planetary Space Sci., 16, 309, 1968.

Hirshberg, J., and D. S. Colburn, Planet. Space Sci., 17, 1183, 1969.

Hirshberg, J., A. Alksne, D. S. Colburn, S. J. Bame, and A. J. Hundhausen, J. Geophys. Res., 75, 1, 1970

Hirshberg, J., S. J. Bame, and D. L. Robbins, Solar Phys., 23, 467, 1972.

Hundhausen, A. J., Solar-Terrestrial Physics/ 1970, Part II, ed., Dyer, D. Reidel, Dordrecht-Holland, 1972a.

Hundhausen, A. J., Coronal Expansion and Solar Wind, Springer-Verlag, New York, 1972b.

Hundhausen, A. J., J. Geophys. Res., 78, 1528, 1973 .

Hundhausen, A. J., and L. F. Burlaga, to be published, 1974.

Hundhausen, A. J., and R. A. Gentry, J. Geophys. Res., 74, 2908, 1967.

Hundhausen, A. J., S. J. Bame, J. R. Asbridge, and S. J. Sydoriak, J. Geophys. Res., 75, 4643, 1970.

Intrilligator, D., Ap. J. (Letters), 188, L28, 1974.

Jones, D. E., J. R. Ballif, and J. G. Melville, J. Geophys. Res., 79, 286, 1974.

Kane, R. P., J. Atmos. Terr. Phys., 34, 1941, 1972.

Kane, R. P., J. Geophys. Res., 79, 64, 1974.

Kovalevsky, J. V., Space Sci. Rev., 12, 187, 1971.

Lewis, R. R., and G. L. Siscoe, J. Geophys. Res., 78, 6443, 1973.

Matsuda, T., and T. Sakurai, Cosmic Electrodynamics, 3, 97, 1972.

Moldovanu, A., Planet. Space. Sci., 22, 193, 1973.

Moldovanu, A., and E.-B. Bradu, Gerlands Beitr. Geophysik, Leipzig 82, 171, 1973.

Montgomery, M., S. J. Bame, and A. J. Hundhausen, J. Geophys. Res., 77, 5432, 1972.

Montgomery, M. D., J. R. Asbridge, S. J. Bame, and W. C. Feldman, J. Geophys. Res., in press, 1974.

Ness, N. F., and J. M. Wilcox, Astrophys. J., 143, 23, 1966.

Ness, N. F., A. J. Hundhausen, and S. J. Bame, J. Geophys. Res., 76, 6643, 1971.

Newton, H. W., M. Not. Roy. Ast. Soc., 103, 244, 1943.

Ogilvie, K. W., Solar Wind, eds., C. P. Sonett, P. J. Coleman, Jr., and J. M. Wilcox, NASA SP-308, p. 430, 1972.

Ogilvie, K. W., and L. F. Burlaga, J. Geophys. Res., in press, 1974.

Ogilvie, K. W., L. F. Burlaga, and T. D. Wilkerson, J. Geophys. Res., 73, 6809, 1968.

Papadopoulos, K. Astrophys. J., 179, 931, 1973.

Papadopoulos, K., R. W. Clark, and C. E. Wagner, Simulation of colliding solar wind streams with multifluid codes, preprint, 1974.

Parker, E. N., Interplanetary Dynamical Processes, Interscience, New York, 1963.

Pizzo, V., J. T. Gosling, A. J. Hundhausen, and S. J. Bame, J. Geophys. Res., 78, 6469, 1973.

Russell, C. T., R. L. McPherron, and R. K. Burton, J. Geophys. Res., 79, 1105, 1974.

Sakurai, T., Cosmic Electrodyn. 1, 460, 1970.

Sari, J. W., Modulation of low energy cosmic rays, NASA/GSFC X-692-72-309, 1972.

Schatten, K. H., and J. E. Schatten, J. Geophys. Res., 77, 4858, 1972.

Scudder, J. D., and L. F. Burlaga, Eos, 55, 413, 1974.

Siscoe, G. L., J. Geophys. Res., 77, 27, 1972.

Siscoe, G. L., and L. T. Finley, J. Geophys. Res., 77, 35, 1972.

Snyder, C. W., Marcia Neugebauer, and V. R. Rao, J. Geophys. Res., 68, 6361, 1963.

Sullivan, J. D., and G. L. Siscoe, Eos, 55, 410, 1974.

Svalgaard, L., Geomagnetic Responses to the solar wind and solar activity, SUIPR Report No. 555, 1973.

Urch, I. H., Cosmic Electrodynamics, 3, 316, 1972.

Wilcox, J. M., and, N. F. Ness, J. Geophys. Res., 70, 5793, 1965.

Yoshida, S., and S.-J. Akasofu, Planet. Space Sci., 14, 979, 1966.

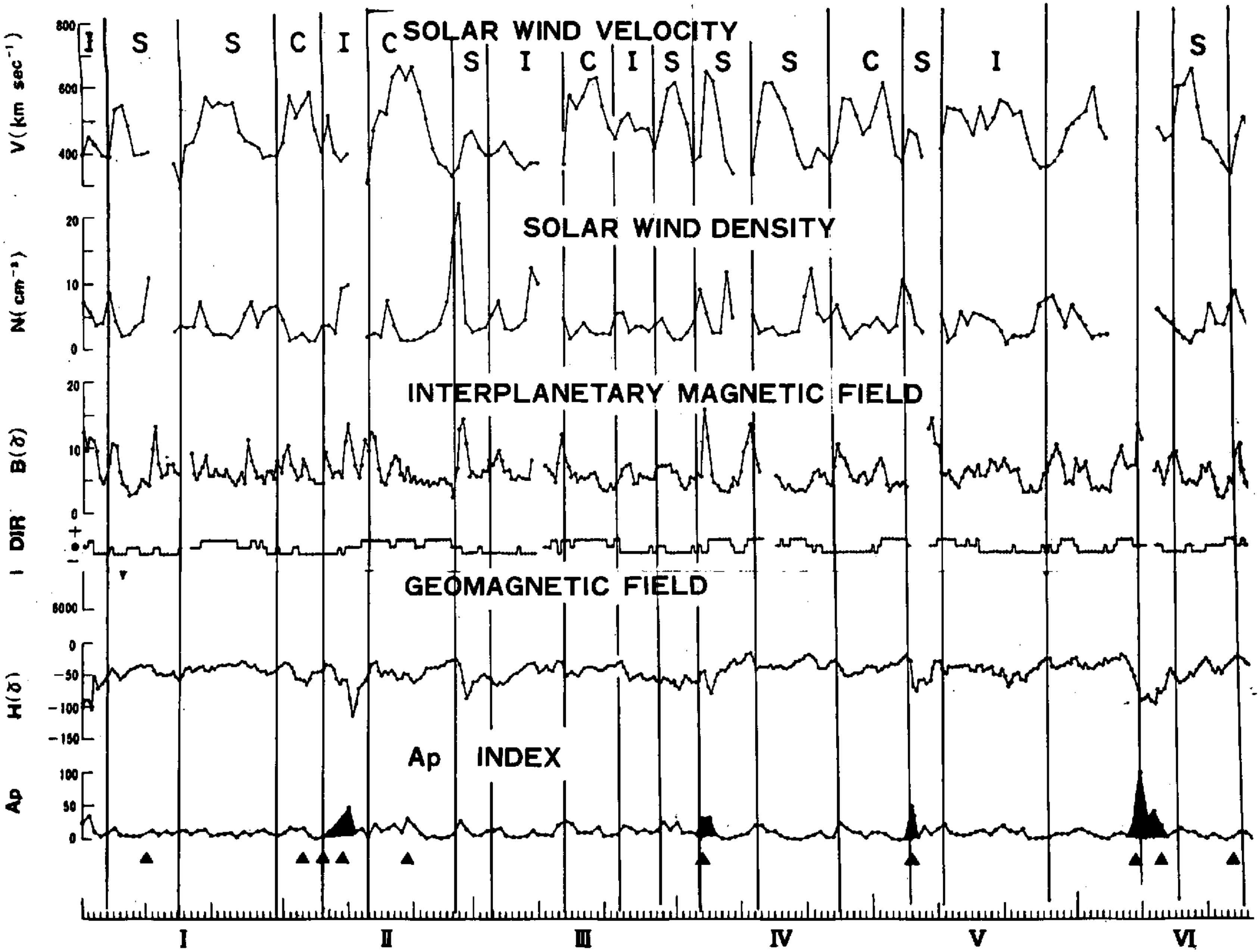
SOLAR WIND VELOCITY
V(km sec⁻¹)
SOLAR WIND DENSITY
N(cm⁻³)
INTERPLANETARY MAGNETIC FIELD
B(γ)
DIR
GEOMAGNETIC FIELD
H(γ)
Ap INDEX
Ap
I
II
III
IV
V
VI

Figure 1

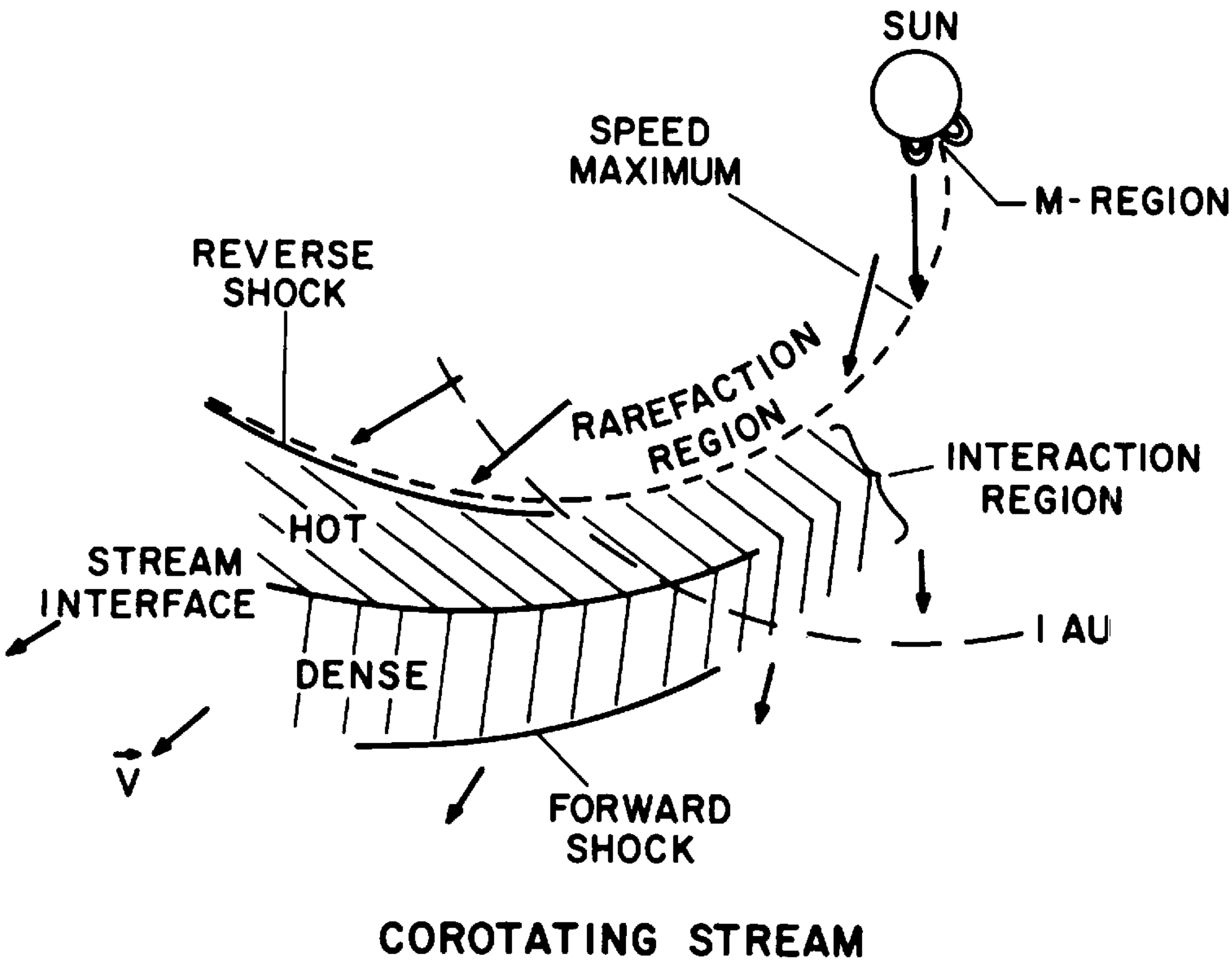
SUN
SPEED
MAXIMUM
M-REGION
REVERSE
SHOCK
RAREFACTION
REGION
INTERACTION
REGION
HOT
STREAM
INTERFACE
I AU
DENSE
V
FORWARD
SHOCK
CORROTATING STREAM

Figure 2

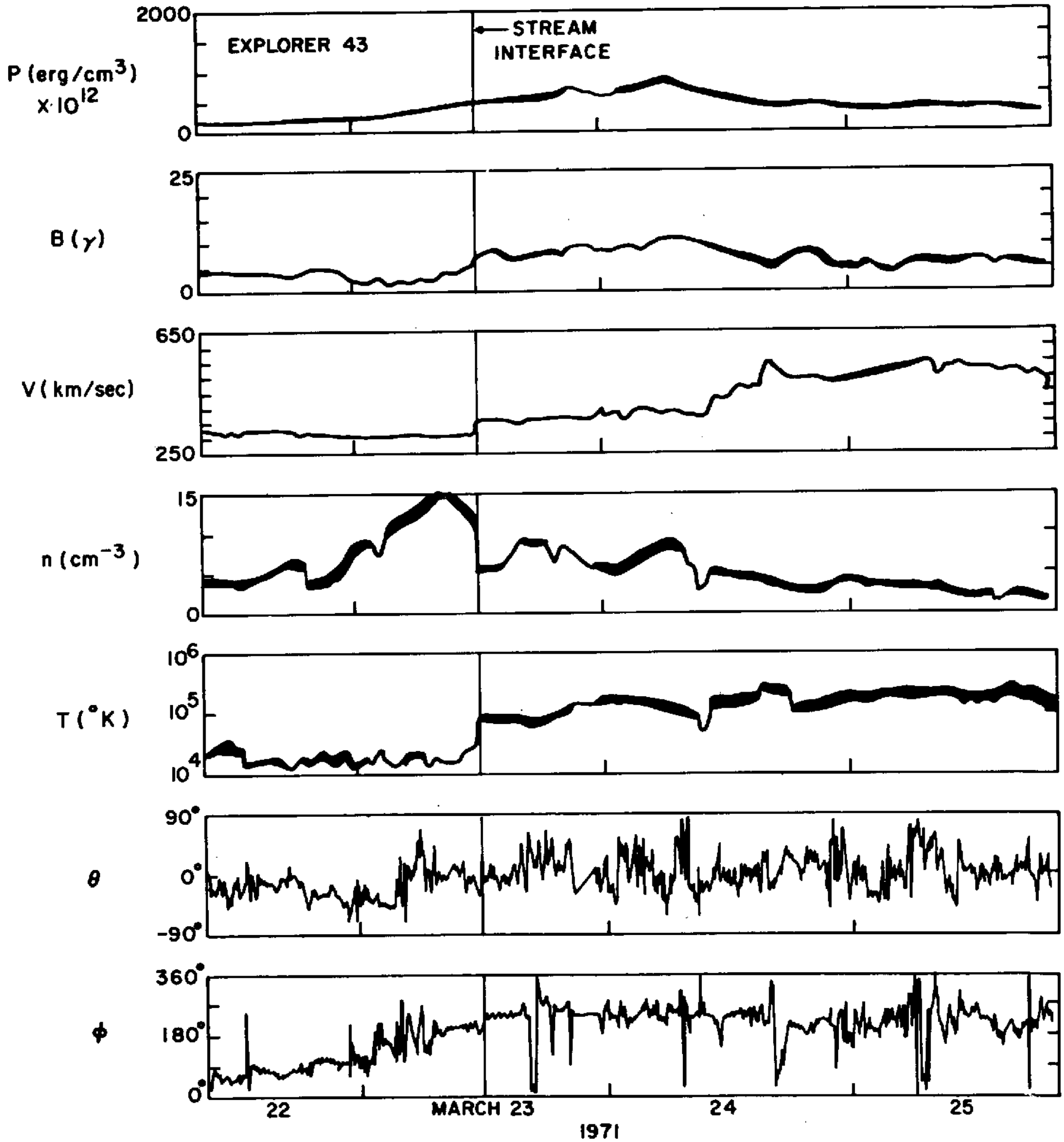

EXPLORER 43
STREAM INTERFACE
P (erg/cm3) X 10^12
2000
0
B (γ)
25
0
V (km/sec)
650
250
n (cm-3)
15
0
T (°K)
10^6
10^5
10^4
θ
90°
0°
-90°
φ
360°
180°
0°
22
MARCH 23
24
25
1971

Figure 3

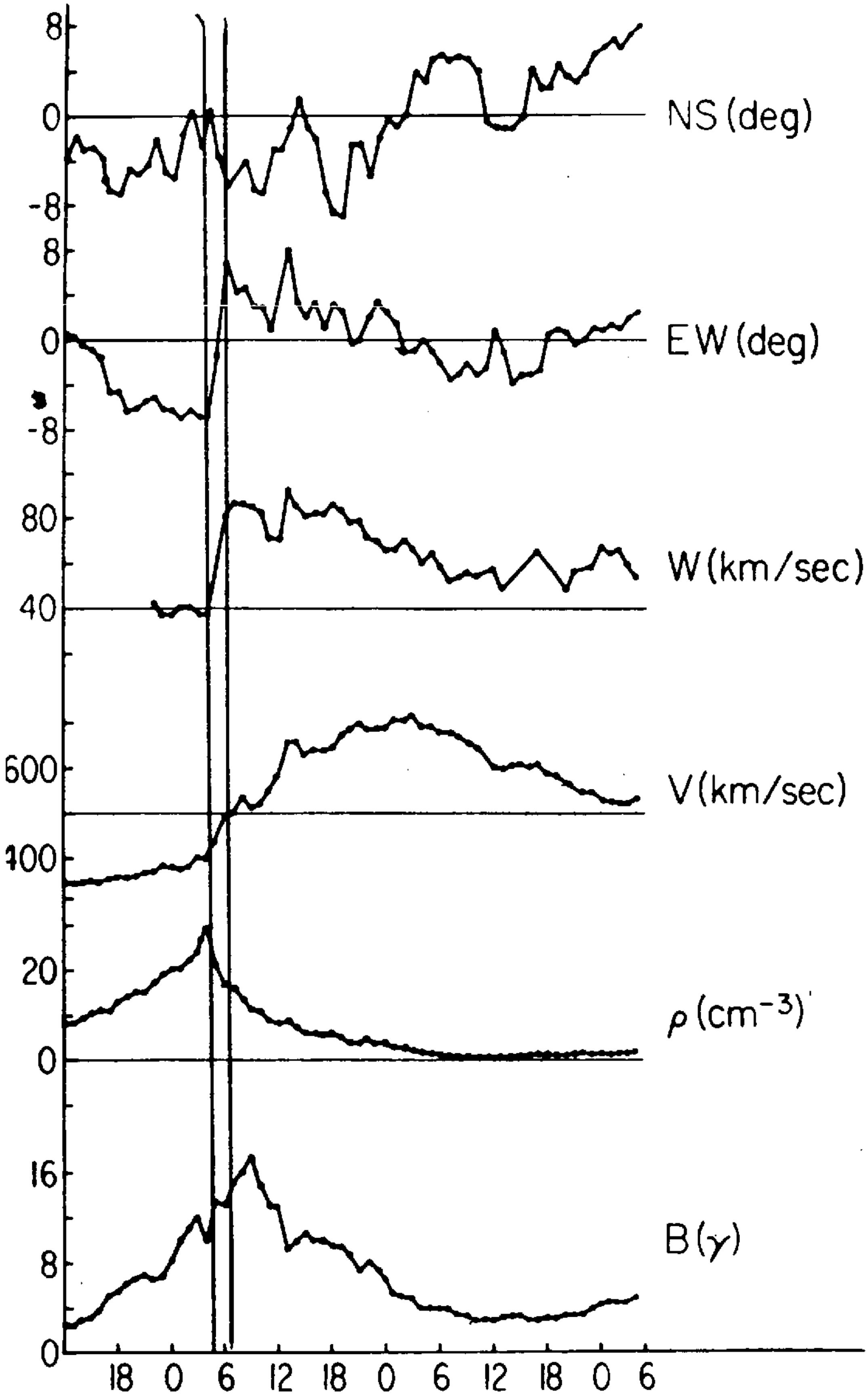
NS (deg)
EW (deg)
W (km/sec)
V (km/sec)
ρ (cm⁻³)
B (γ)
8
0
-8
8
0
-8
80
40
600
400
20
0
16
8
0
18 0 6 12 18 0 6 12 18 0 6
2/19/66

Figure 4

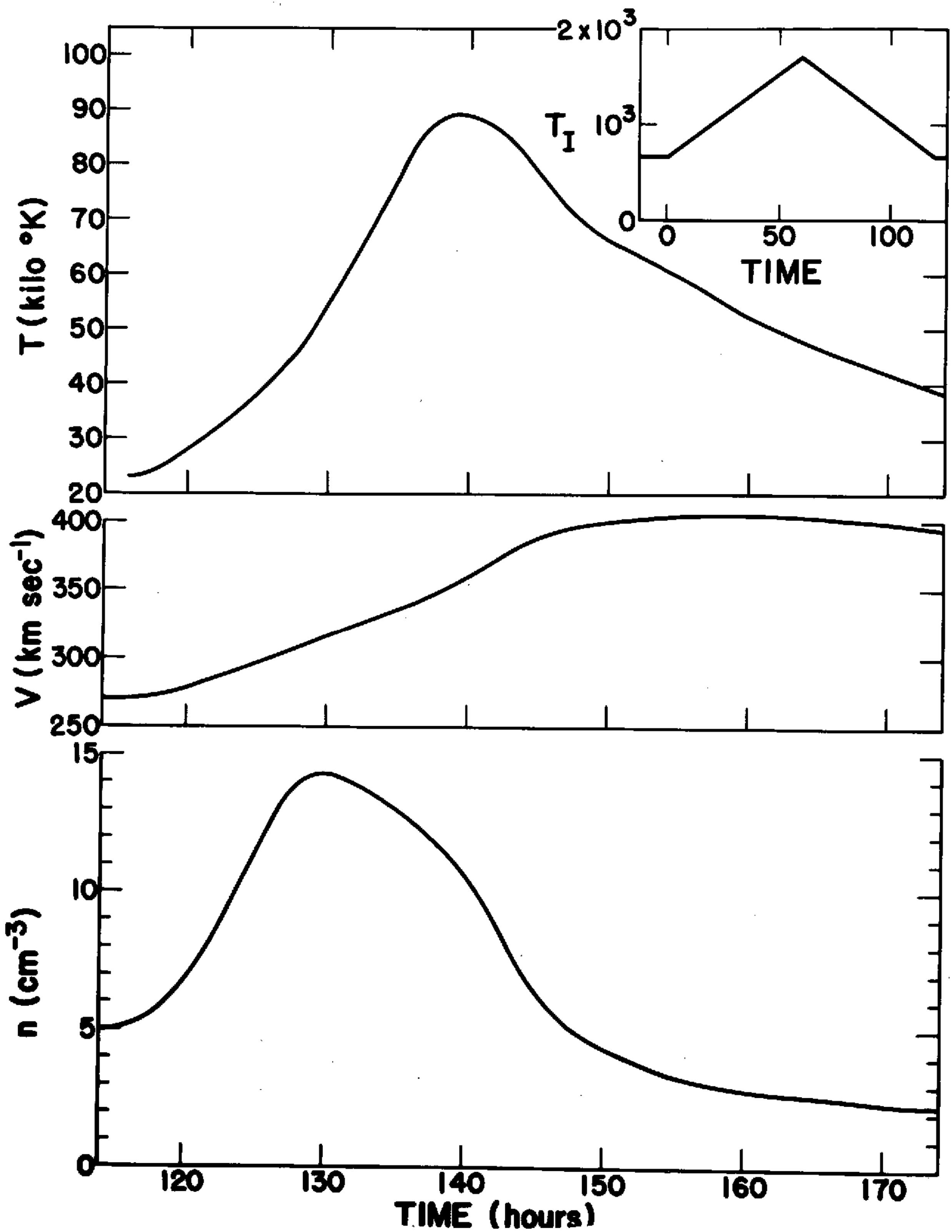

T (kilo °K)
100
90
80
70
60
50
40
30
20
T_I
2×10^3
10^3
0
0
50
100
TIME
V (km sec^{-1})
400
350
300
250
n (cm^{-3})
15
10
5
0
120
130
140
150
160
170
TIME (hours)

Figure 5

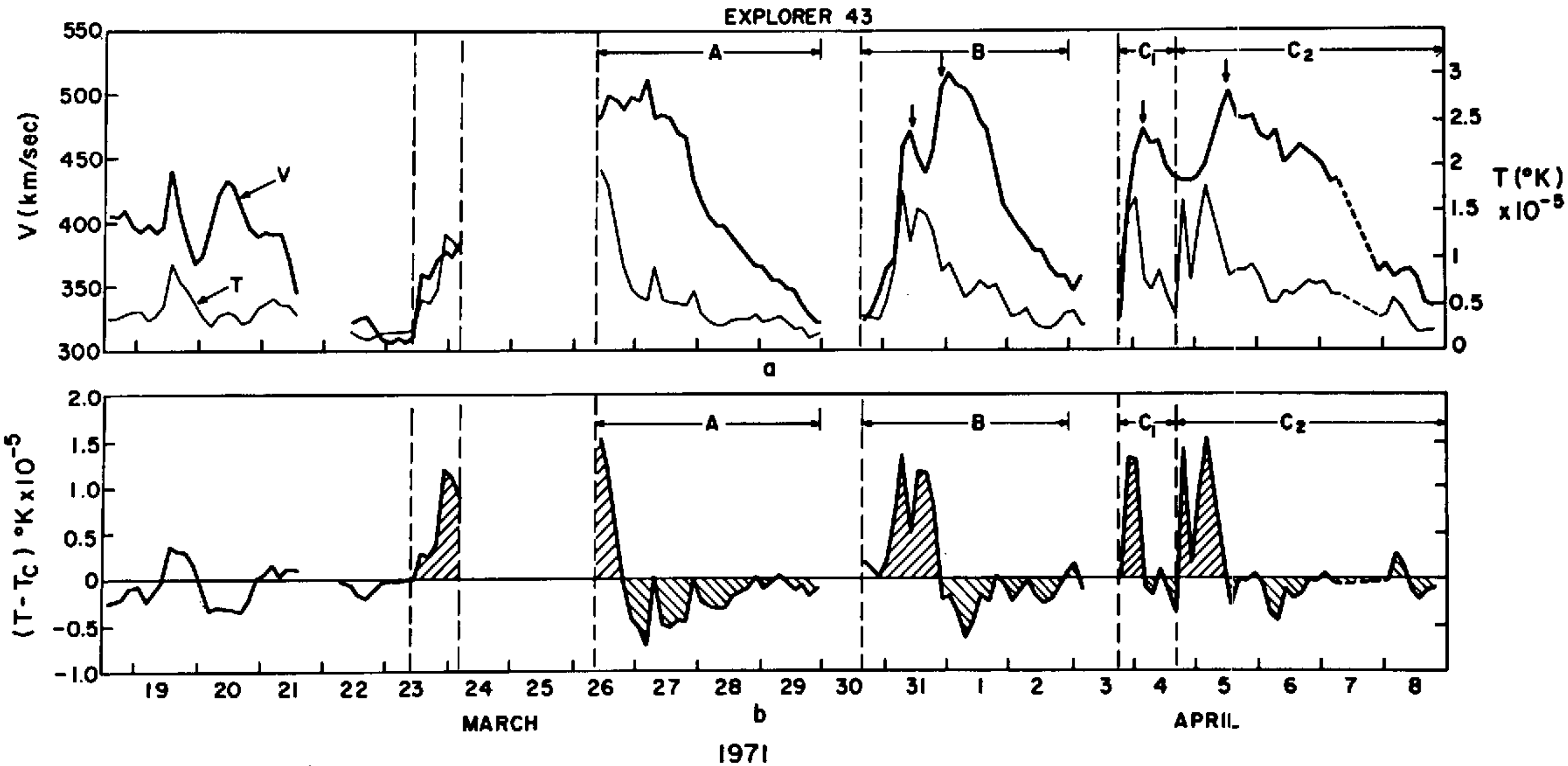
EXPLORER 43
V (km/sec)
T (°K) x10⁻⁵
V
T
A
B
C₁
C₂
a
(T - T_C) °K x10⁻⁵
b
MARCH
APRIL
1971

Figure 6

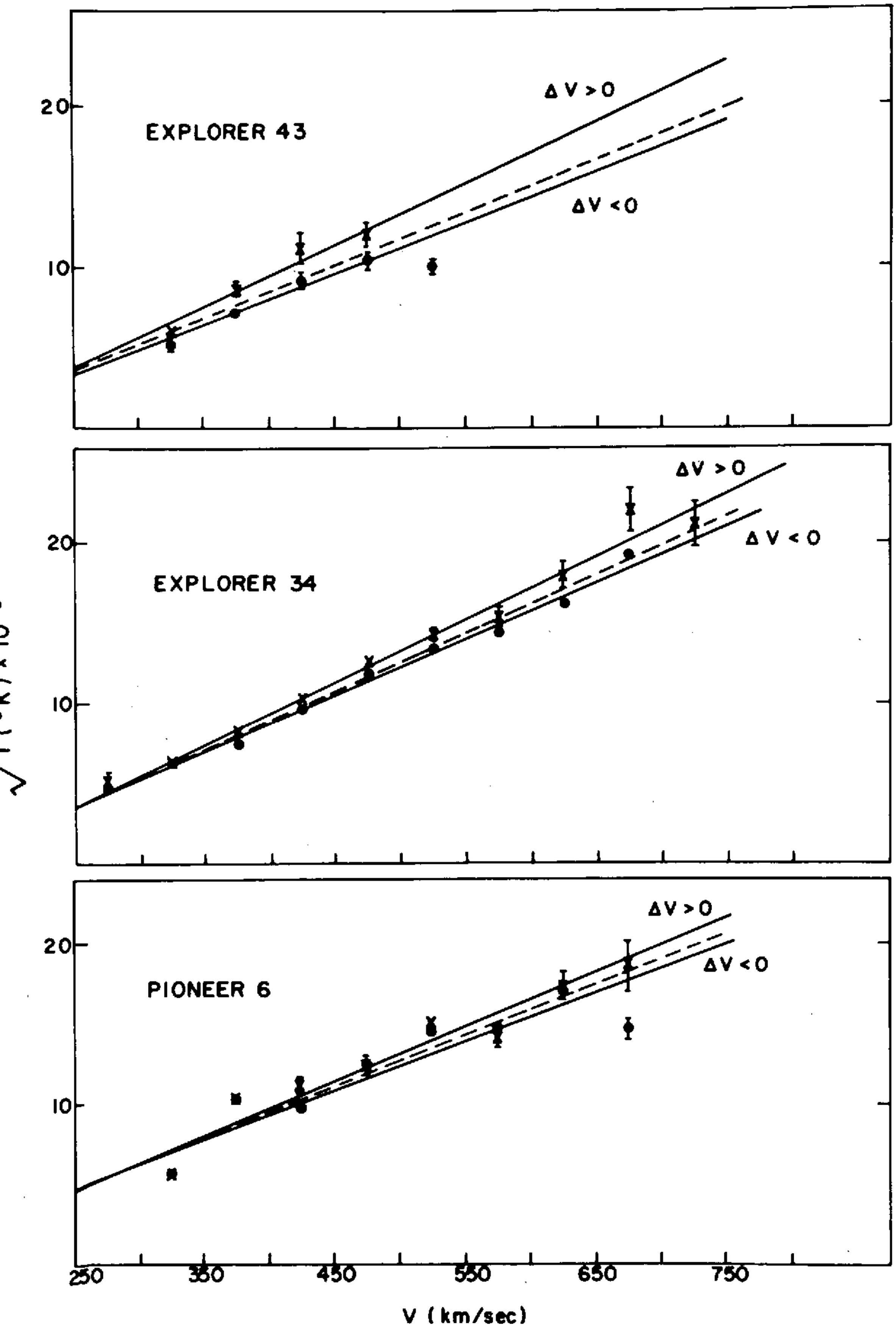
EXPLORER 43
ΔV > 0
ΔV < 0
EXPLORER 34
ΔV > 0
ΔV < 0
PIONEER 6
ΔV > 0
ΔV < 0
$\sqrt{T\,(^\circ K)} \times 10^{-3}$
20
10
250
350
450
550
650
750
V (km/sec)

Figure 7

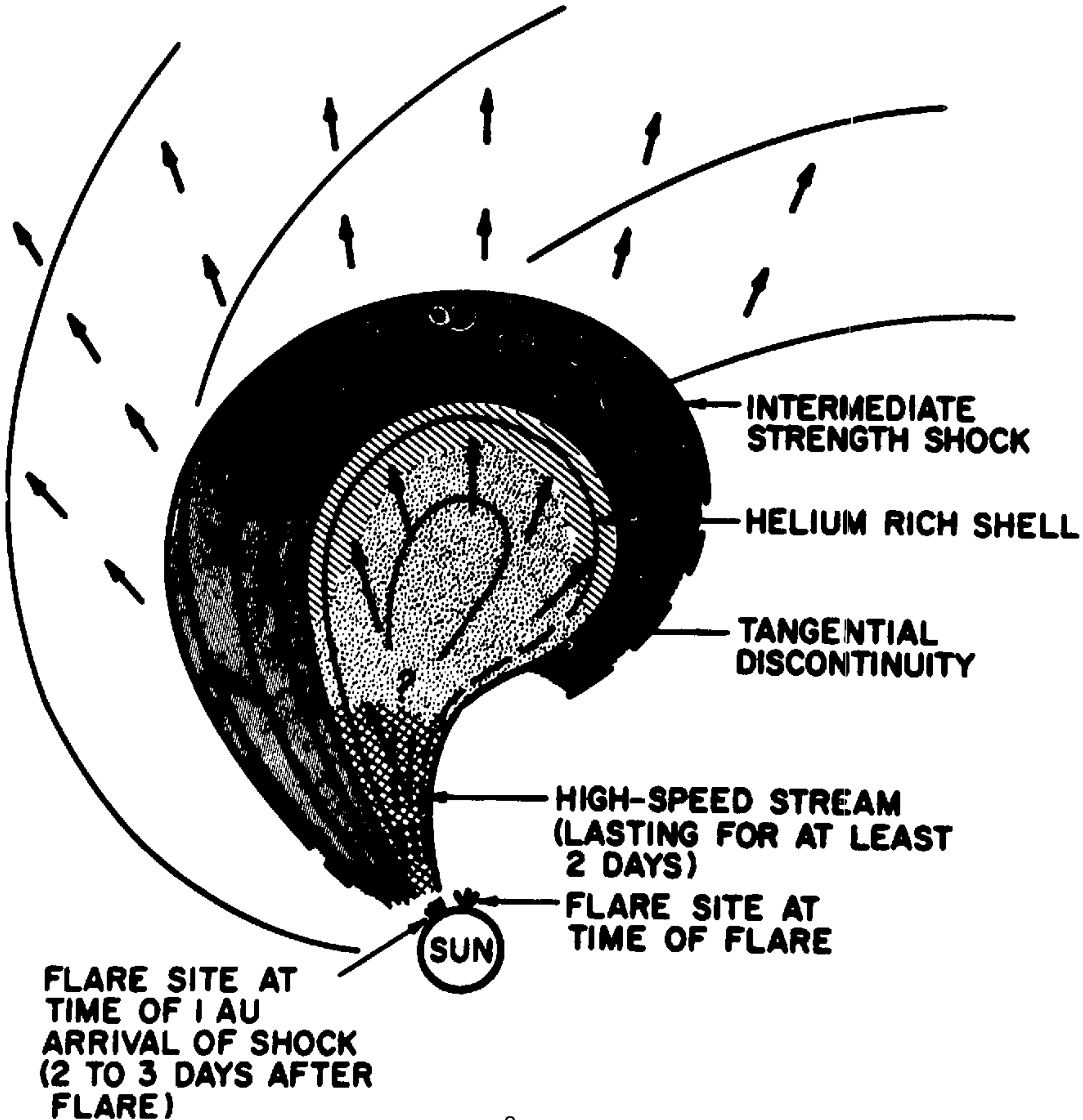
INTERMEDIATE STRENGTH SHOCK
HELIUM RICH SHELL
TANGENTIAL DISCONTINUITY
HIGH-SPEED STREAM (LASTING FOR AT LEAST 2 DAYS)
FLARE SITE AT TIME OF FLARE
SUN
FLARE SITE AT TIME OF I AU ARRIVAL OF SHOCK (2 TO 3 DAYS AFTER FLARE)

Figure 8

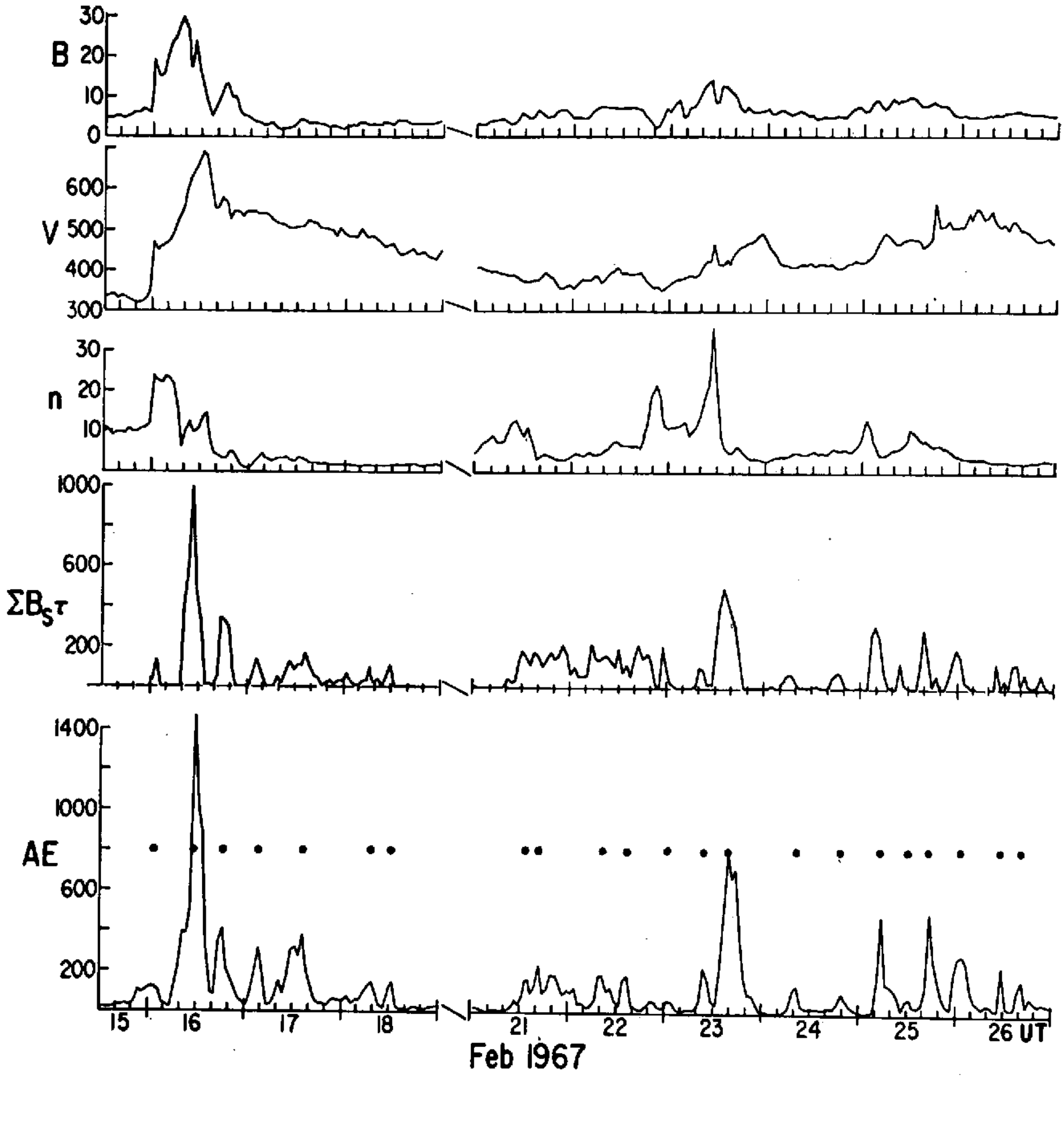
B
30
20
10
0
V
600
500
400
300
n
30
20
10
1000
600
$\Sigma B_s\tau$
200
1400
1000
AE
600
200
15
16
17
18
21
22
23
24
25
26 UT
Feb 1967

Figure 9

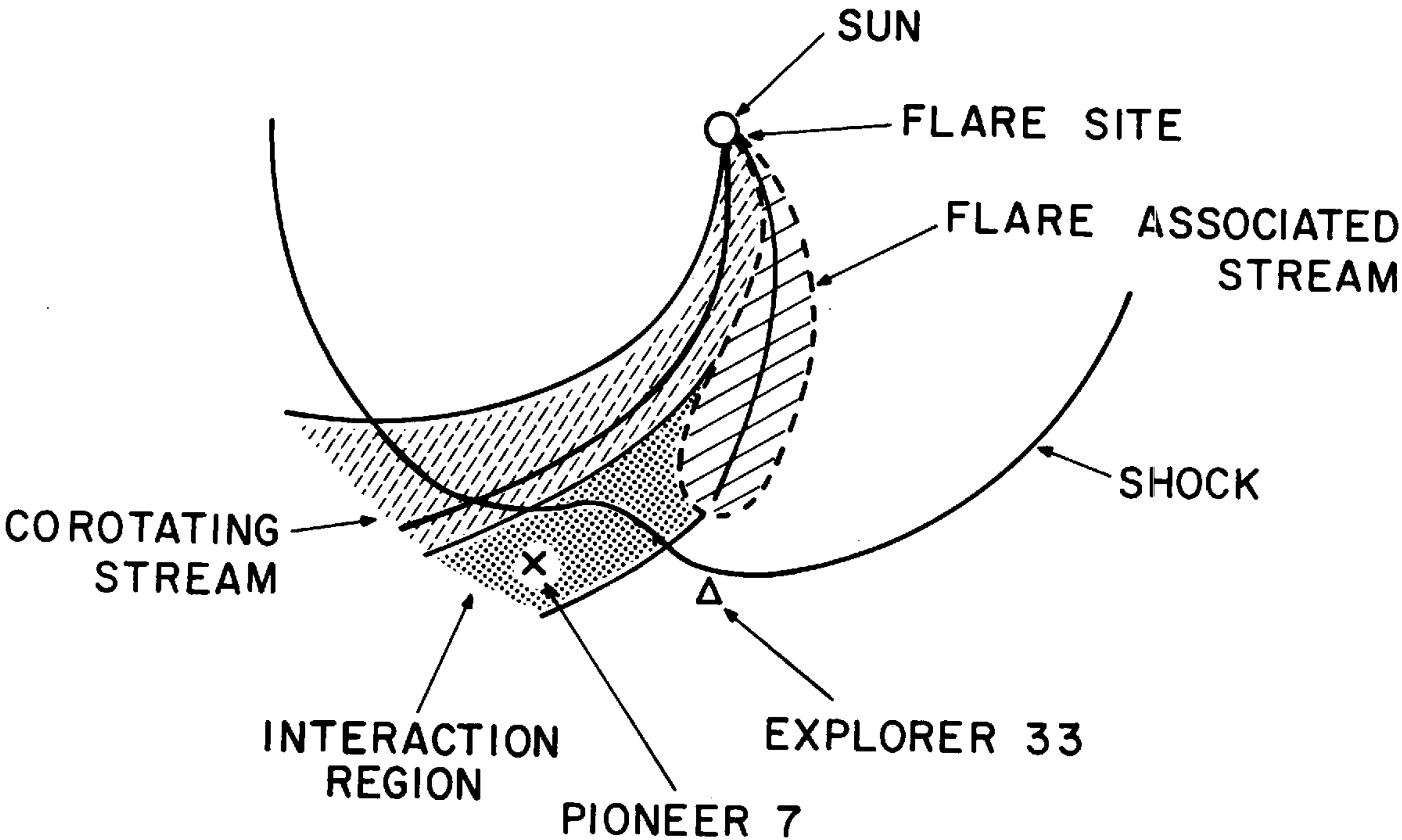
SUN
FLARE SITE
FLARE ASSOCIATED STREAM
SHOCK
COROTATING STREAM
INTERACTION REGION
PIONEER 7
EXPLORER 33

Figure 10

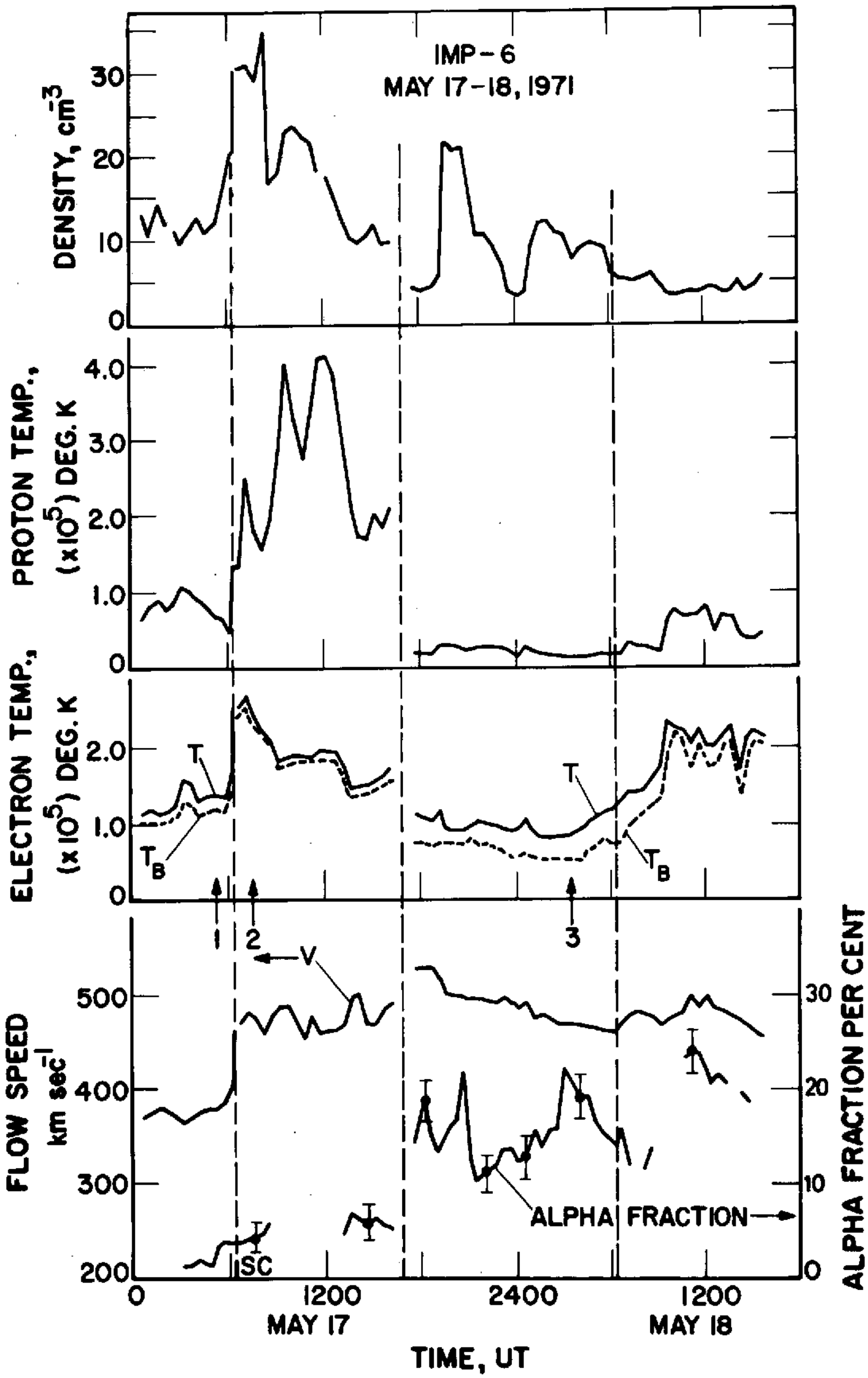
IMP-6
MAY 17-18, 1971
DENSITY, cm^{-3}
PROTON TEMP., (x10^5) DEG. K
ELECTRON TEMP., (x10^5) DEG. K
T
T_B
1
2
3
V
FLOW SPEED km sec^{-1}
ALPHA FRACTION
ALPHA FRACTION PER CENT
SC
0
1200
2400
MAY 17
MAY 18
TIME, UT

Figure 11

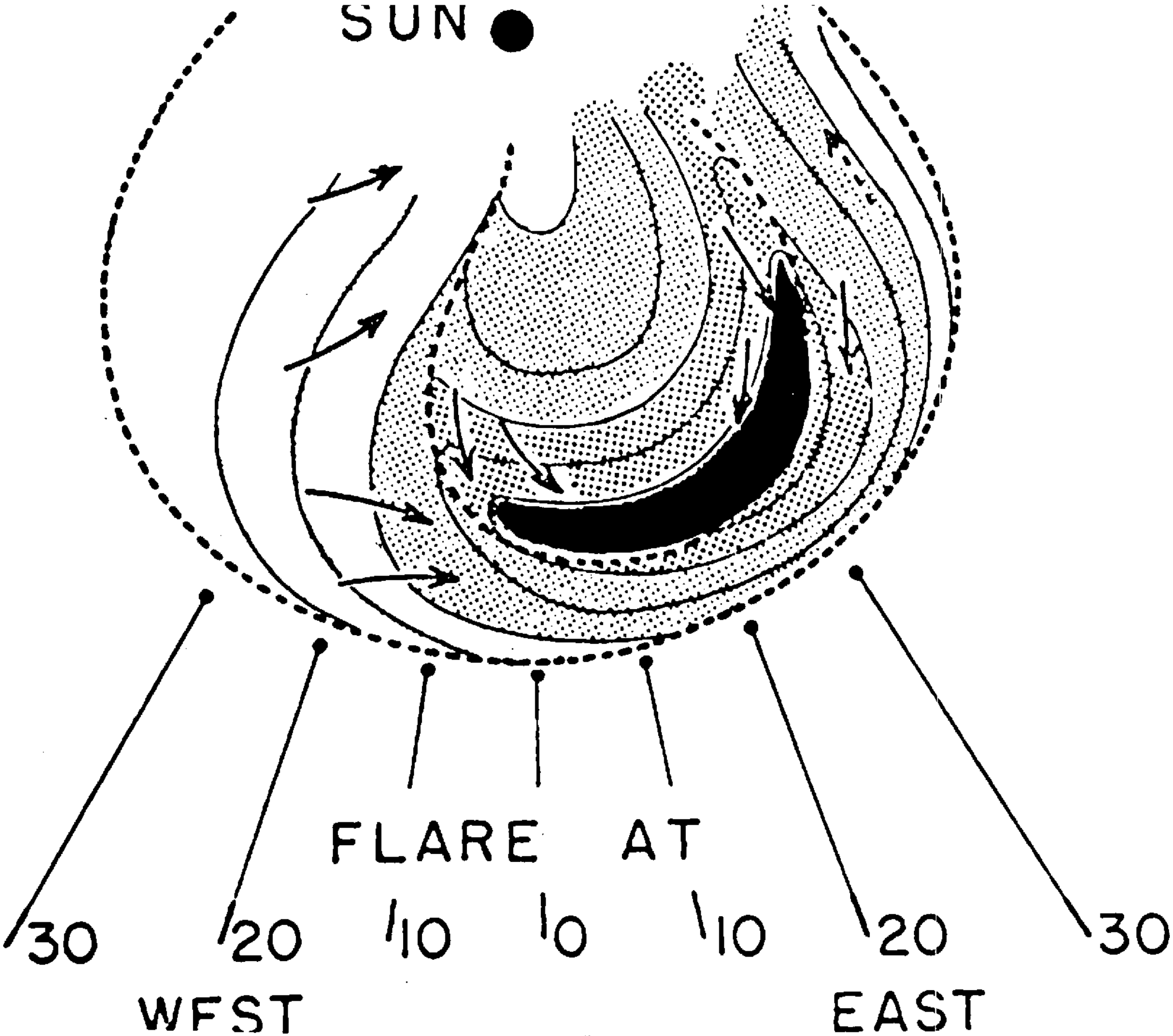

Figure 12

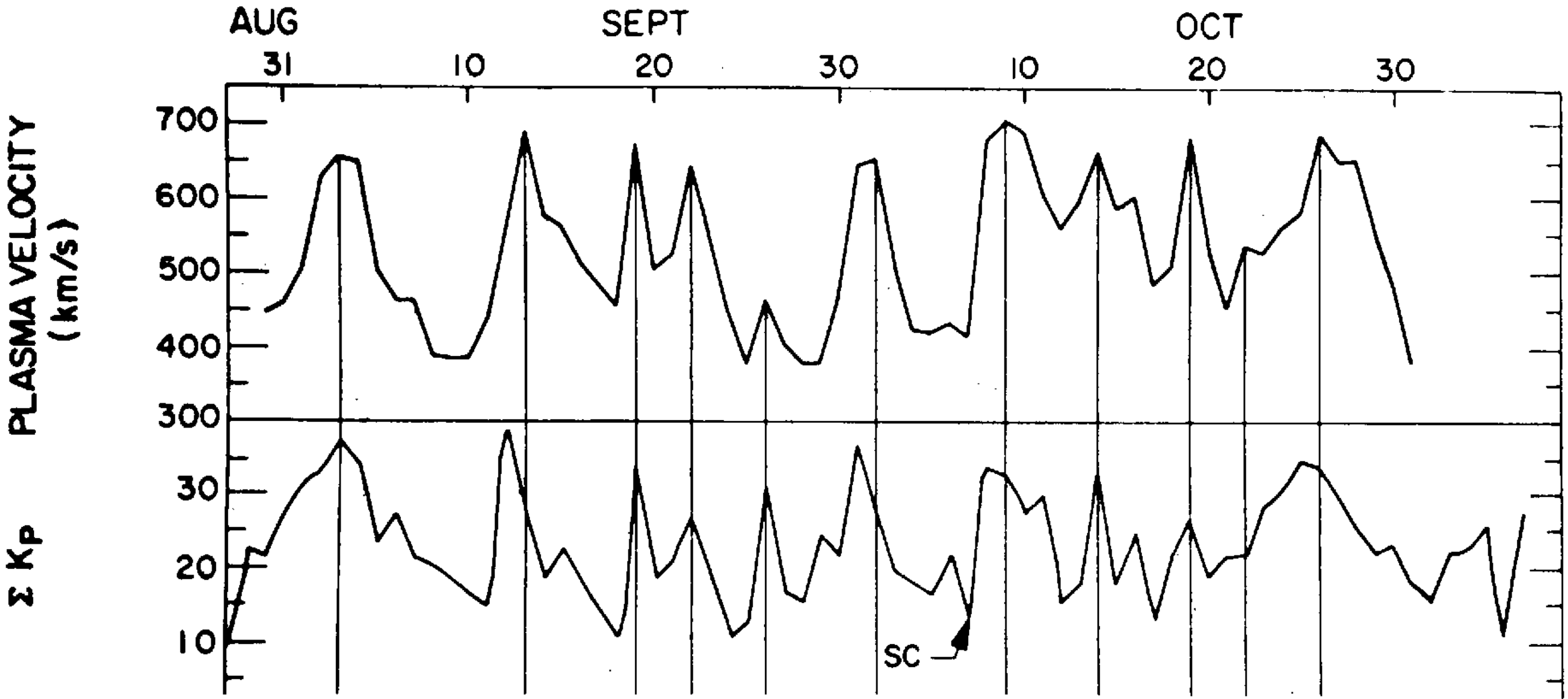
AUG
SEPT
OCT
31
10
20
30
10
20
30
PLASMA VELOCITY (km/s)
700
600
500
400
300
Σ K_P
30
20
10
SC

Figure 13

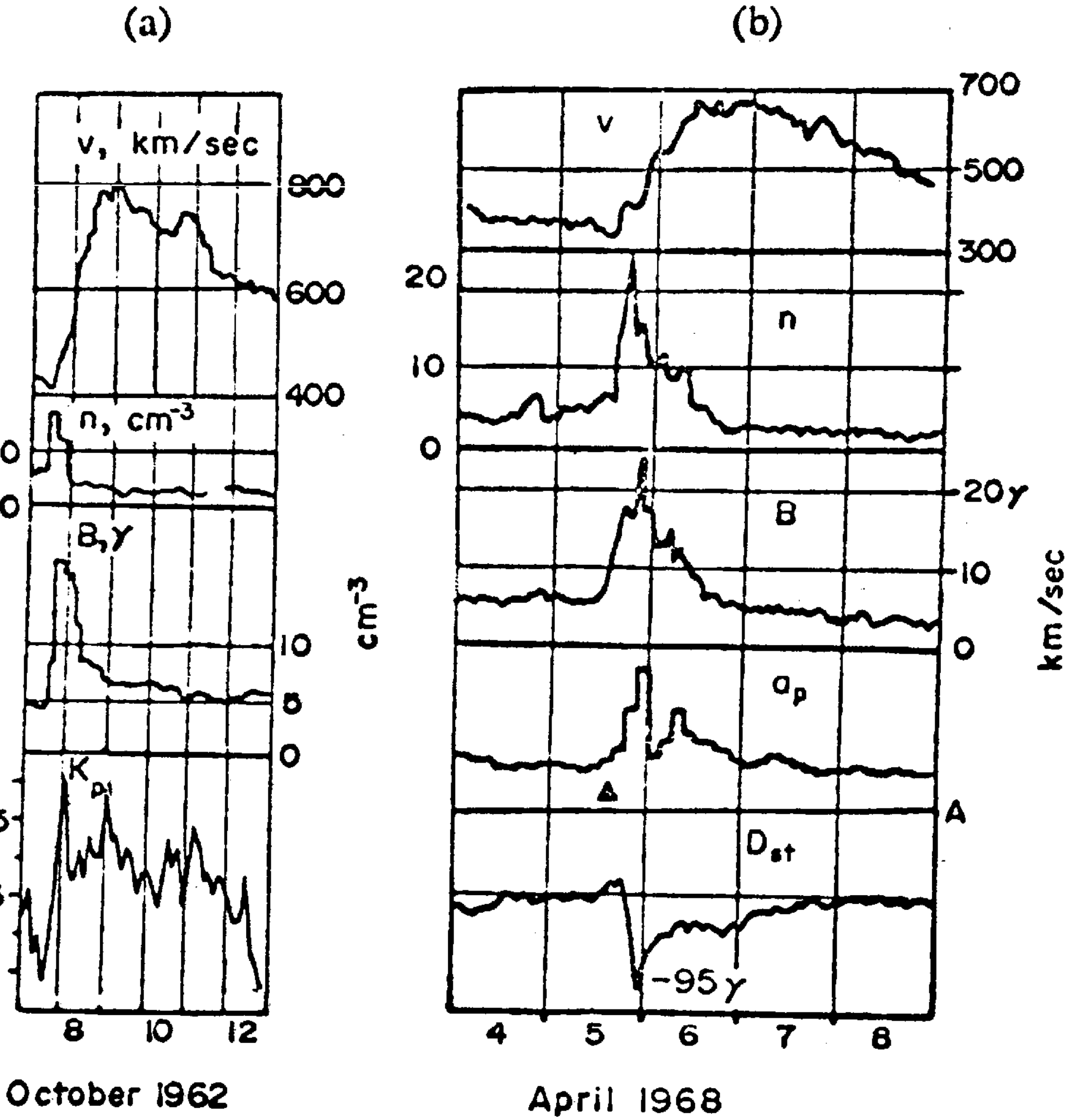
(a)
(b)
v, km/sec
800
600
400
n, cm^{-3}
20
0
B, γ
10
5
0
K_{p1}
5
3
1
8
10
12
October 1962
cm^{-3}
v
700
500
300
n
20
10
0
B
20 γ
10
0
a_p
A
D_{st}
−95 γ
4
5
6
7
8
April 1968
km/sec

Figure 14

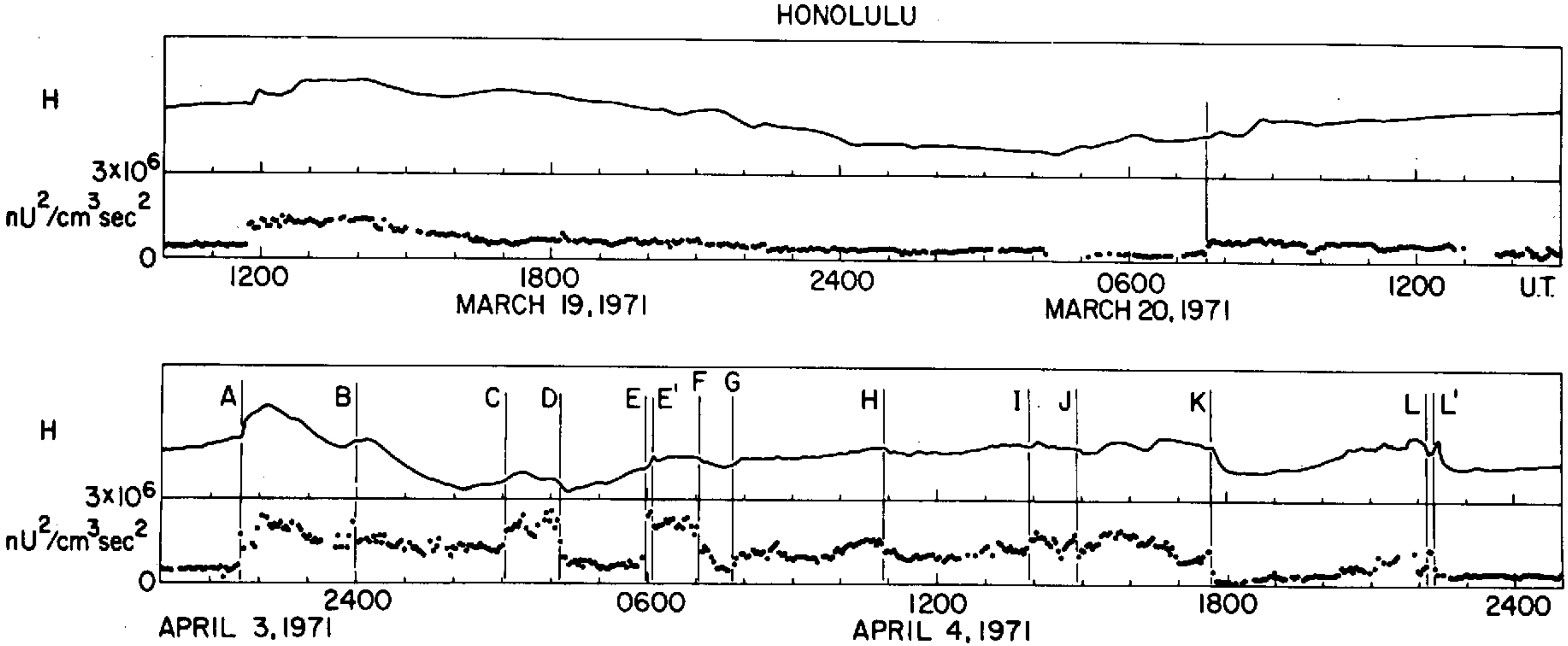

HONOLULU
H
3x10^6
nU^2/cm^3sec^2
0
1200
1800
2400
0600
1200
U.T.
MARCH 19, 1971
MARCH 20, 1971
A
B
C
D
E
E'
F
G
H
I
J
K
L
L'
H
3x10^6
nU^2/cm^3sec^2
0
2400
0600
1200
1800
2400
APRIL 3, 1971
APRIL 4, 1971

Figure 15

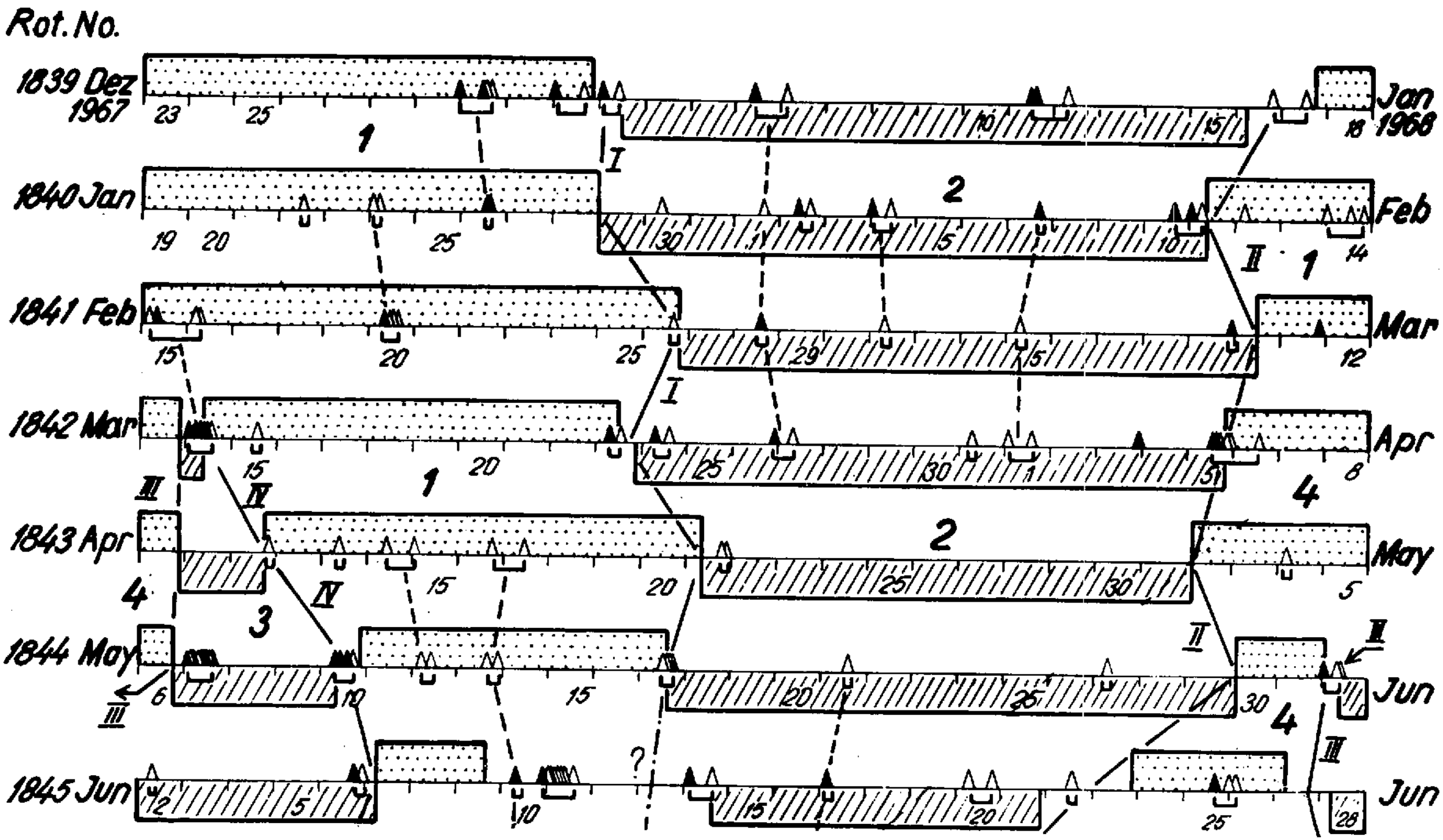
Rot. No.
1839 Dez
1967
Jan
1968
1840 Jan
Feb
1841 Feb
Mar
1842 Mar
Apr
1843 Apr
May
1844 May
Jun
1845 Jun
Jun

Figure 16

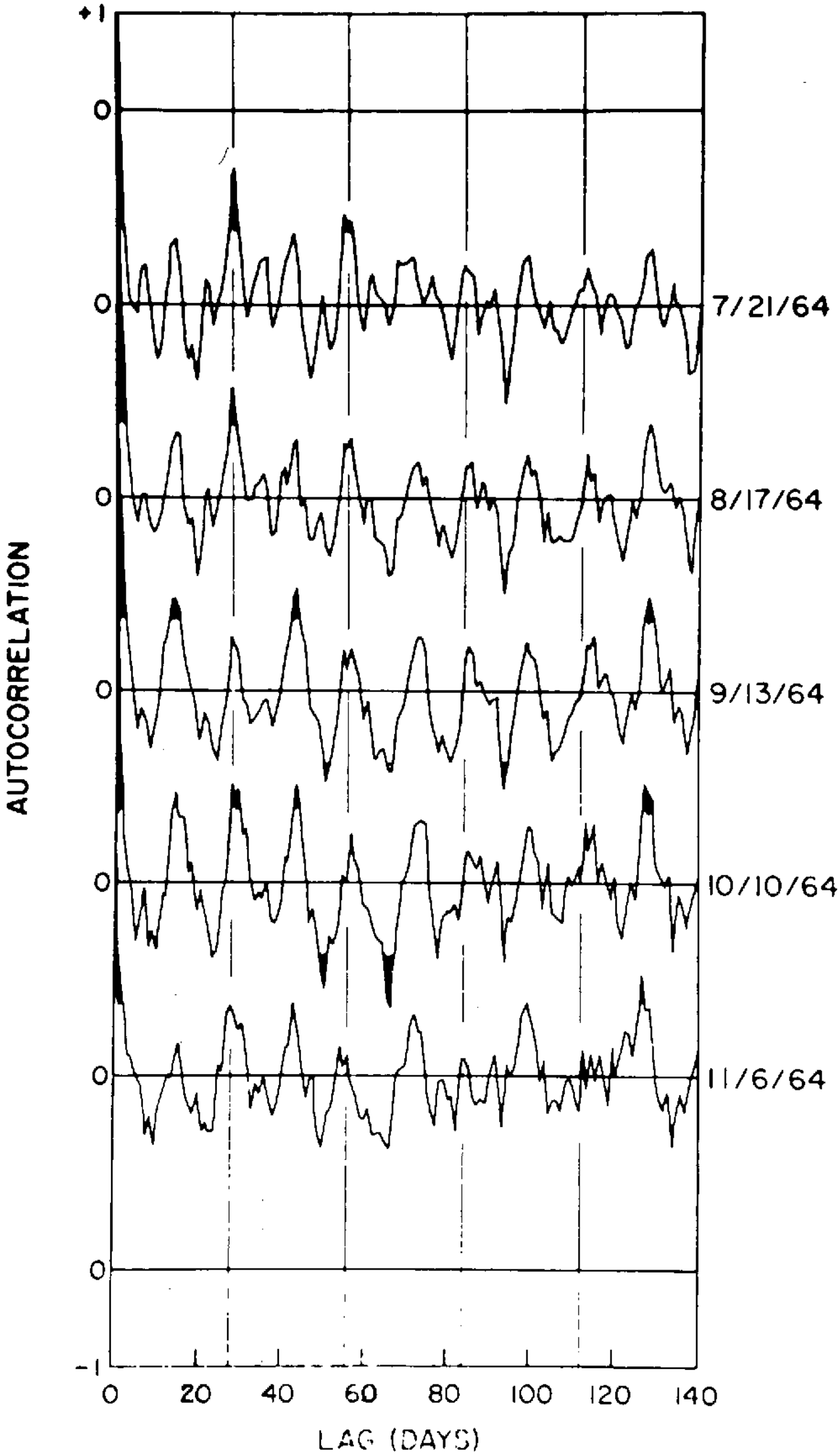

AUTOCORRELATION
+1
0
0
7/21/64
0
8/17/64
0
9/13/64
0
10/10/64
0
11/6/64
0
-1
0
20
40
60
80
100
120
140
LAG (DAYS)

Figure 17

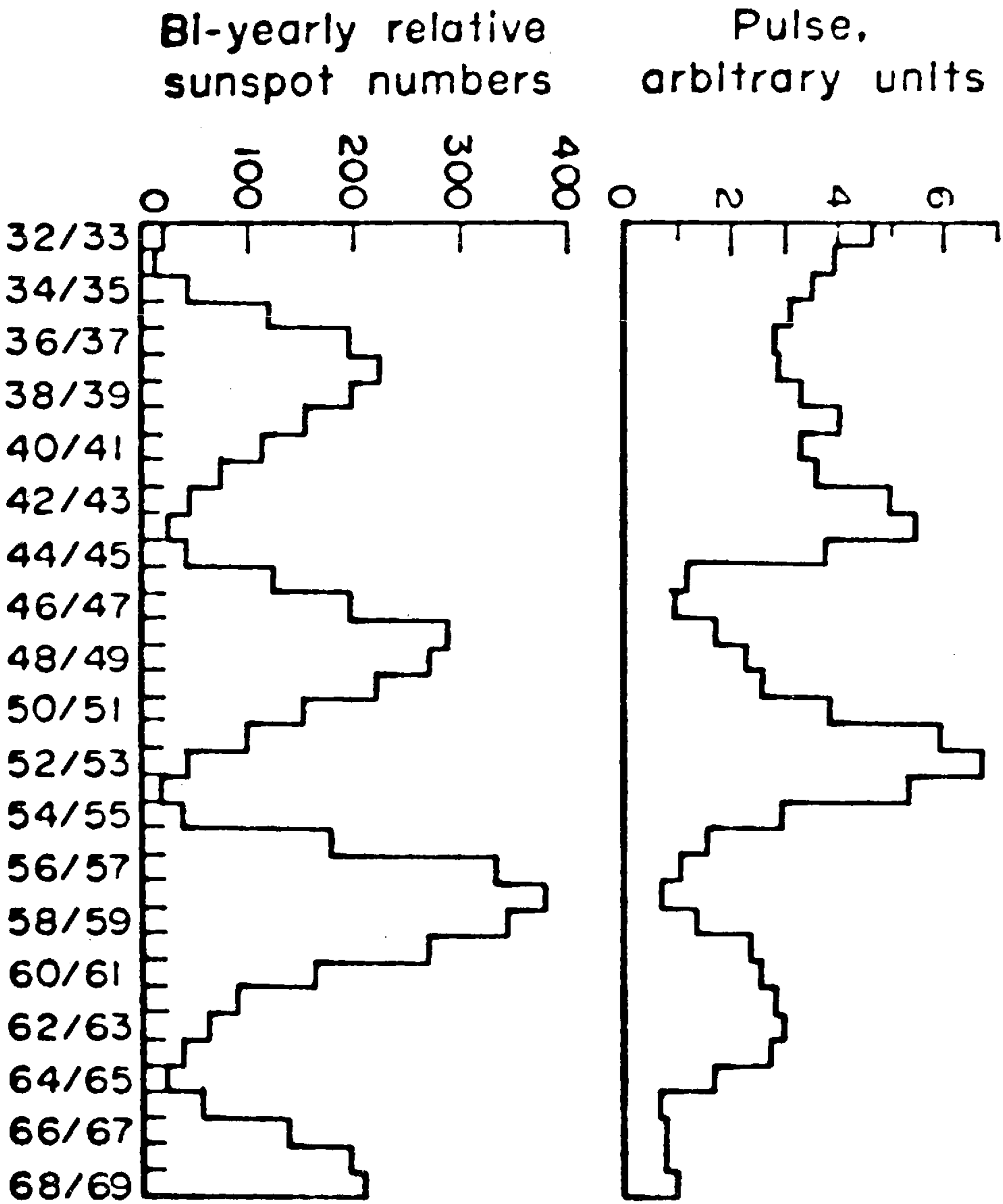

BI-yearly relative sunspot numbers
Pulse, arbitrary units
0
100
200
300
400
0
2
4
6
32/33
34/35
36/37
38/39
40/41
42/43
44/45
46/47
48/49
50/51
52/53
54/55
56/57
58/59
60/61
62/63
64/65
66/67
68/69

Figure 18